RR 257

Research Report 257
THE EQUATION OF STATE OF ICE AND COMPOSITE FROZEN SOIL MATERIAL

by
Gordon D. Anderson

JUNE 1968

U.S. ARMY MATERIEL COMMAND
COLD REGIONS RESEARCH & ENGINEERING LABORATORY
HANOVER, NEW HAMPSHIRE

Sta[illegible]rd Research Institute
Contract DAAG 23-67-0011

6

Research Report 257

THE EQUATION OF STATE OF ICE AND COMPOSITE FROZEN SOIL MATERIAL

by

Gordon D. Anderson

JUNE 1968

U.S. ARMY MATERIEL COMMAND
COLD REGIONS RESEARCH & ENGINEERING LABORATORY
HANOVER, NEW HAMPSHIRE

Stanford Research Institute
Contract DAAG 23-67-0011

DA Task 1T025001A13001

PREFACE

The work reported here was performed by the Poulter Laboratory for High Pressure Research of Stanford Research Institute under Contract DAAG 23-67-0011 with the U.S. Army Cold Regions Research and Engineering Laboratory (USA CRREL). This research was supported by the Advanced Research Projects Agency of the Department of Defense and was monitored by USA CRREL under ARPA Order 968.

The study was a project of the Experimental Engineering Division (Mr. K.A. Lineil, Chief) USA CRREL. The project leader was Dr. G.D. Anderson of Stanford Research Institute and the USA CRREL project monitors were Mr. A.F. Wuori (Chief, Applied Research Branch) and Mr. E. Chamberlain. The participation of the following staff members of Stanford Research Institute is gratefully acknowledged: Mr. A.L. Fahrenbruch and Mr. R.W. Gates for explosive shot designs and firing and sample preparation; Mr. C.F. Allen, Mr. R.E. Aumiller, and Mr. L.J. Dary for shot construction; Mr. J.E. Vargo and Mr. G.S. Cartwright for test site operations; and Miss B.Y. Loo for data analysis.

USA CRREL is an Army Materiel Command laboratory.

CONTENTS

FIGURES

TABLES

NOMENCLATURE

n	porosity
s	saturation
t	time
u	particle velocity at any position
u_1	final particle velocity behind shock
U	shock velocity
u_{fs}	free-surface velocity
V	specific volume at any position
V_o	initial specific volume
V_1	final specific volume behind shock
x	position (Eulerian coordinate)
ρ	density at any position
ρ_o	initial density
ρ_1	final density behind shock
ρ_d	initial dry density of soil sample
ρ_t	total initial density of soil sample
ρ_x	crystal density
σ	normal stress at any position
σ_o	initial normal stress
σ_1	final normal stress behind shock
ξ	characteristic steady state coordinate $\xi = x - Ut$
w	percent water of soil sample based on dry weight

SUMMARY

The U.S. Army Cold Regions Research and Engineering Laboratory (USA CRREL) is participating in a program concerned with the computation of shock wave propagation in frozen soil-water mixtures. To perform such computations it is necessary to know a constitutive relation or an equation of state of the medium under consideration. Shock wave techniques provide a powerful tool for the investigation of equations of state at very high stress levels. The task of investigating the stress-volume behavior of frozen soil-water mixtures in the range from 60 to 500 kbar was undertaken by Stanford Research Institute at the request of USA CRREL.

Hugoniot data were obtained for Ottawa banding sand (pure quartz sand) and West Lebanon (New Hampshire) glacial till of varying degrees of saturation and for polycrystalline and monocrystalline ice (c-axis oriented in the direction of shock propagation). Release cross curve data were obtained for dry and saturated Ottawa banding sand and for polycrystalline ice. All materials were at an initial temperature of -10°C. In all experiments plane one-dimensional shock waves were used. The Hugoniots and release curves for the soil materials show evidence of a quartz-stishovite phase transition at about 300 kbar. The Hugoniots of single and polycrystalline ice do not differ significantly over the stress range studied--30 kbar to 300 kbar.

INTRODUCTION

In order to predict shock wave propagation and attenuation it is generally necessary to know a constitutive relation or an equation of state of the medium in which the waves are propagating. In some applications a single Hugoniot curve* is sufficient, since it predicts the velocity at which a pressure pulse of a given amplitude will propagate. It also predicts the impedance of the medium relative to media which may bound it. In order to predict the rate at which a given shock wave is attenuated because of being overtaken by rarefactions, it is necessary to know the unloading paths the material follows in releasing from various pressures. Both the loading and unloading paths can be determined using shock wave techniques.

The objective of the work reported here was to obtain Hugoniot curves in the pressure range from 60 to 500 kbar for Ottawa sand and West Lebanon glacial till of varying degrees of saturation, and in the pressure range from 30 to 300 kbar for ice. Release adiabat data were obtained for dry and saturated Ottawa sand and for polycrystalline ice. All materials studied were at an initial temperature of -10°C.

---

* The Hugoniot curve is defined as the locus of final states that can be reached from a given initial state by a shock transition. The locus is commonly presented as a curve in the stress-volume, stress-particle velocity, or shock velocity-particle velocity plane.

TECHNICAL BACKGROUND

Rankine-Hugoniot Shock Equations

Consider a plane, one-dimensional, steady-state, compressional wave propagating in the positive x direction at a constant velocity U in a continuous medium. The profile of the wave at a given instant of time is shown schematically in Fig. 1. The component of the normal stress in the direction of propagation of the wave, the density, and the particle velocity are denoted by σ, ρ, and u, respectively. Prior to the arrival of the wave front the material is at a stress σ_o, a density ρ_o, and at rest ($u = 0$). After the compressional wave passes over an element of the material it is assumed to be in a final equilibrium state in which it will remain. The final state is characterized by $\sigma = \sigma_1$, $\rho = \rho_1$, and $u = u_1$. Between the initial and final equilibrium states the material undergoes a continuous change in the variables σ, ρ, and u. The existence of such a steady state must be assumed a priori. The conditions under which a steady state may exist have been studied by others (Bethe, 1942).

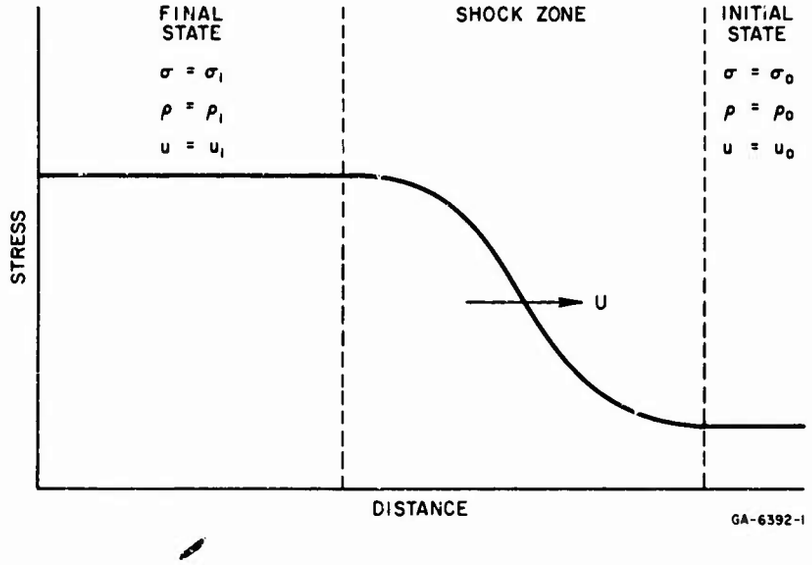

FIG. 1 STRESS PROFILE OF A SHOCK WAVE

The partial differential equations that describe general time-dependent, plane, one-dimensional flow in a continuum are:

$$\frac{\partial \rho}{\partial t} + \frac{\partial}{\partial x}(\rho u) = 0 \qquad (1)$$

and

$$\frac{\partial \sigma}{\partial x} + \rho\left(\frac{\partial u}{\partial t} + u\frac{\partial u}{\partial x}\right) = 0 \quad . \qquad (2)$$

Equation (1) expresses the conservation of mass and Eq. (2) expresses the conservation of momentum. Since the flow is a steady state it will appear unchanged in time if it is observed from a frame of reference moving at a velocity U (the shock velocity). This means that the variables σ, ρ, and u are all functions of the single variable $\xi = x - Ut$. The partial derivative operators then become

$$\frac{\partial}{\partial x} = \frac{d}{d\xi}\,; \qquad \frac{\partial}{\partial t} = -U\frac{d}{d\xi} \quad . \qquad (3)$$

Equations (1) and (2) become, for a steady-state flow,

$$\frac{d}{d\xi}[\rho(U - u)] = 0 \qquad (1a)$$

and

$$\frac{d\sigma}{d\xi} - \rho(U - u)\frac{du}{d\xi} = 0 \quad . \qquad (2a)$$

Integration of Eq. (1a) yields

$$\rho(U - u) = \text{constant} \quad . \qquad (4)$$

If the boundary condition from the initial state is $\rho = \rho_o$ when $u = 0$, it follows that the constant is $\rho_o U$. Equation (4) then becomes

$$\rho(U - u) = \rho_o U \quad . \qquad (4a)$$

The boundary condition from the final state (that $\rho = \rho_1$ when $u = u_1$) could have been used, and the two boundary conditions would yield

$$\rho_o U = \rho_1(U - u_1) \quad . \qquad (4b)$$

Equation (4b) relates the density and particle velocity of the initial state to the density and particle velocity of the final state. (This equation is generally referred to as the Rankine-Hugoniot mass equation.) From Eq. (4a) it is clear that in a steady-state profile the mass equation applies not only to the initial and final states, but also to any state in the interior of the profile, i.e., in the shock zone (see Fig. 1).

Equation (4a) may be combined with Eq. (2a) to yield

$$\frac{d}{d\xi} (\sigma - \rho_o U u) = 0 \qquad (5)$$

which upon integration becomes

$$\sigma = \sigma_o + \rho_o U u \qquad (5a)$$

where again we have the boundary condition $\sigma = \sigma_o$ when $u = 0$. Equation (5a) relates the stress and particle velocity within the shock zone to the initial state. Since it also applies to the final state we can write

$$\sigma_1 = \sigma_o + \rho_o U u_1 \quad . \qquad (5b)$$

Equation (5b) relating the initial and final states is the Rankine-Hugoniot momentum jump condition for the shock. As in the case of the mass equation, the momentum equation (5a) relates the stress and particle velocity within the shock zone to the end states in the case of a steady state profile.

The shock itself is characterized by the variables relating to the initial and final equilibrium states, while the thickness and shape of the shock zone are governed by the time scale of the irreversible processes occurring as the material is shocked from the initial to the final state. If the irreversible processes occur infinitely fast, the shock zone shrinks to zero thickness (i.e., it becomes a discontinuity). There are then only the initial and final states, which are related by Eqs. (4b) and (5b). In the case of a discontinuity the assumption of steady state is no longer necessary to establish the validity of the jump conditions.

The conservation of mass and momentum equations, (4b) and (5b), are two equations that relate the three variables behind the shock, σ_1, ρ_1, and u_1, to the initial state. It is assumed that the shock velocity U is known. For a simple system the shock velocity uniquely defines the shocked state, so a third relation must exist between the initial and final states. This third relation is the Hugoniot of the material. Equations (4b) and (5b) express the basic kinematic and dynamic principles of a steady-state flow. However, they say nothing of the thermodynamics of the flow nor do they reflect any material properties of the medium. This information is contained in the Hugoniot, which is obtained by combining the energy-stress-strain equation of state of the material with the equation of conservation of energy. We have shown that in the steady-state case the conservation of mass and momentum equations hold throughout the shock zone, which contains nonequilibrium states. The Hugoniot relation, on the other hand, refers only to the initial and final equilibrium states. The Hugoniot may be represented symbolically by stating one of the four shock variables, U, σ_1, ρ_1, or u_1 as a function of one of the others for a given initial state. Common choices are:

$$U = U(u_1), \qquad \sigma_1 = \sigma_1(u_1), \qquad \sigma_1 = \sigma_1(V_1)$$

where $V_1 = 1/\rho_1$, the final specific volume.

The Rayleigh Line

The two equations expressing conservation of mass and momentum in a steady-state shock profile have been shown to be

$$\rho_o U = \rho(U - u) \tag{4a}$$

and

$$\sigma = \sigma_o + \rho_o U u \quad . \tag{5a}$$

For a given steady state shock profile, σ, ρ, and u vary through the profile so that:

$$\sigma_o \leq \sigma \leq \sigma_1 \quad ,$$

$$\rho_o \leq \rho \leq \rho_1 \quad ,$$

and

$$0 \leq u \leq u_1 \quad .$$

However, the shock velocity U is constant <u>for a given shock</u>. Equation (5a) states that in the stress-particle velocity plane, all of the states within the shock zone lie on a straight line of slope $\rho_o U$ and intercept σ_o (see Fig. 2). Measurement of the constant velocity of a steady state shock

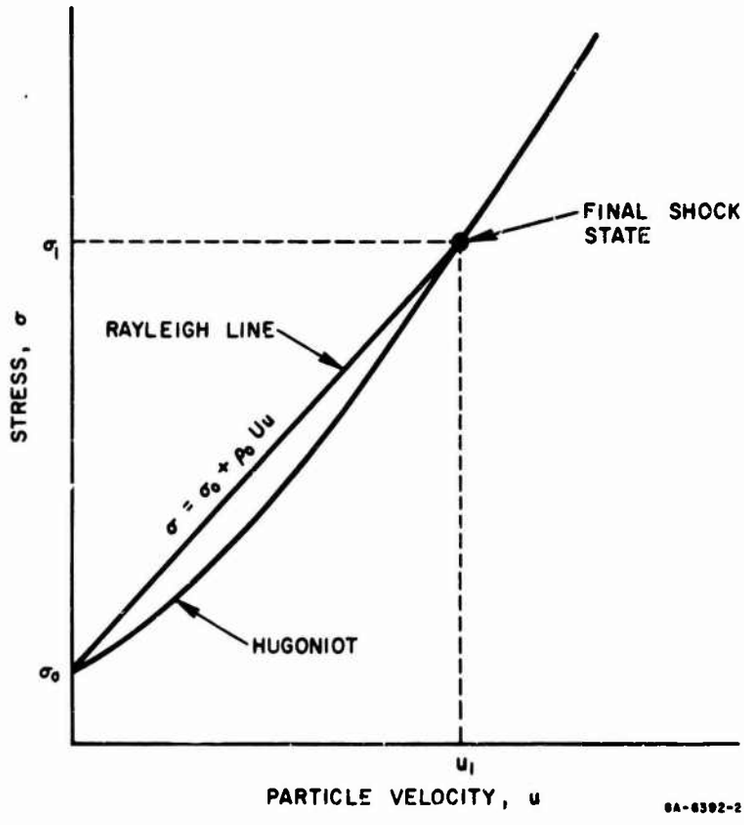

FIG. 2 HUGONIOT AND RAYLEIGH LINE IN STRESS-PARTICLE VELOCITY PLANE

yields the slope, $\rho_o U$. This straight line, commonly referred to as the Rayleigh line, therefore plays an important role in the measurement of Hugoniot curves of different materials by shock wave techniques. The intercept σ_o is known from the initial state of the material. However, to determine which point on the Rayleigh line corresponds to the final state behind the shock, the Hugoniot curve must be known. In the stress-particle velocity plane the Hugoniot is given symbolically by $\sigma_1 = \sigma_1(u_1)$. Recall that the Hugoniot curve refers only to the final state. The final state is then given by the intersection of the Rayleigh line and the Hugoniot curve, as this is the only point that satisfies both Eq. (5a) and $\sigma_1 = \sigma_1(u_1)$.

Elimination of u between Eqs. (4a) and (5a) yields

$$\sigma = \sigma_o + \rho_o U^2 - \rho_o^2 U^2 V = \sigma_o + \rho_o U^2 \left(1 - \frac{V}{V_o}\right) \qquad (6)$$

where V is the specific volume. In the stress-volume plane, the Rayleigh line is again a straight line of slope $-\rho_o^2 U^2$. The final state behind the shock is given by the intersection of the Rayleigh line and the Hugoniot curve $\sigma_1 = \sigma_1(V_1)$ (see Fig. 3).

For a particular material there is one Hugoniot curve for a given initial state that represents the locus of final states that can be reached from that initial state by a shock transition. For each steady-state shock of different intensity (final stress), there is a different Rayleigh line whose slope depends upon the shock velocity. The final state is given by the intersection of the Rayleigh line and the Hugoniot. The intermediate states (states within the shock zone), however, all lie along the Rayleigh line.

Release Cross Curves

The stress-particle velocity plane is perhaps the most useful in reducing the data from shock wave experiments. This is because of the boundary condition that, when a shock wave propagates across an interface bounding two media, the normal component of the stress and the particle velocity are continuous across the interface. The Hugoniots in the stress-

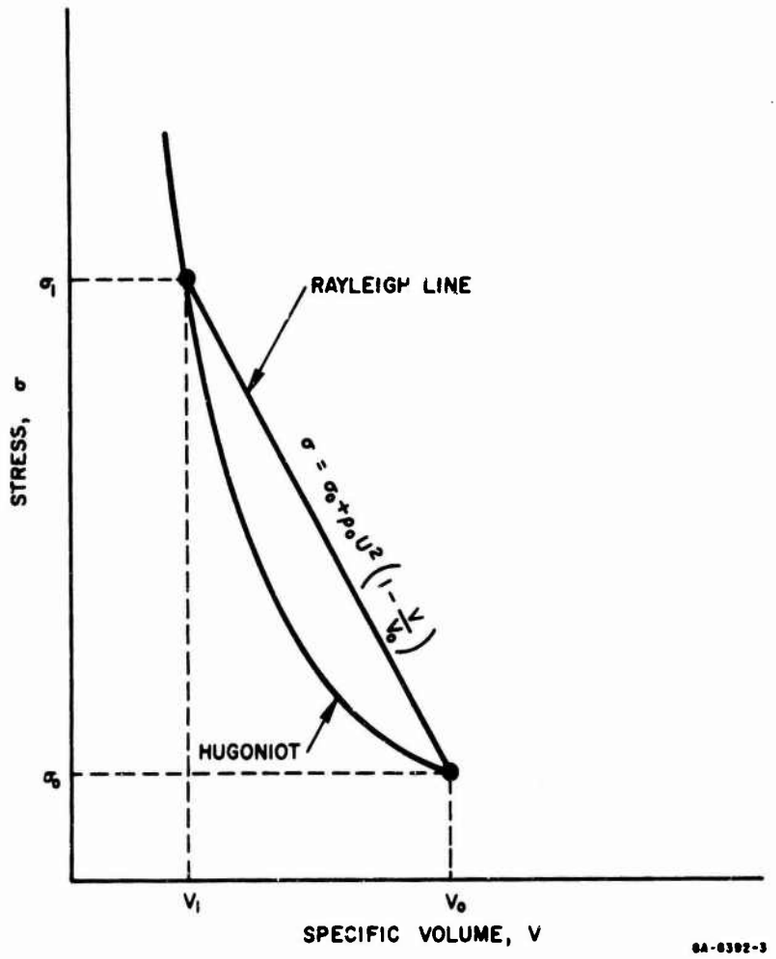

FIG. 3 HUGONIOT AND RAYLEIGH LINE IN STRESS–SPECIFIC VOLUME PLANE

particle velocity plane of two different materials (labeled I and II) are shown schematically in Fig. 4. These Hugoniots represent the loci of final stress-particle velocity states that can be reached in the materials by shocks propagating in the positive x direction into materials initially at rest. Here, σ_o has been set equal to zero because, when dealing with solids, the initial stress (one atmosphere), is negligible compared to the final stress, which is frequently several kilobars.* The Hugoniots representing the loci of states reached by a shock propagating in the negative x direction into material at rest would be these same curves reflected through the σ axis. If the material were initially in motion the appropriate curves would be translated to the left or right along the u axis by an amount equal to the magnitude of the initial velocity. The positions of the curves in the stress-particle velocity plane represent the kinematics of the problem, whereas the positions of the curves in the stress-volume plane do not.

Let us now consider only the case of shocks propagating in the positive x direction into media at rest. The final states lie on the curves I and II shown in Fig. 4. The shock impedance of a material is defined as $Z_s = \rho_o U$, the slope of the Rayleigh line. Since the shock velocity depends upon the final stress in the wave, the shock impedance is also a function of the final stress. For the two materials represented in Fig. 4, the shock impedance of material I is greater than that of material II at a given pressure. Suppose now that a steady-state profile propagating in material I arrives at a free surface. The boundary condition is that the free surface is always at a state of zero stress. At the time that the foot of the profile reaches the free surface, the steady state ceases to exist. A thin layer of material (of the thickness of the shock zone) adjacent to the free surface is never shocked to the final state σ_1, ρ_1, u_1. These particles are at intermediate states lying along the Rayleigh line. Because of the stress gradient, the free surface begins to accelerate and a rarefaction wave begins to propagate back into the profile, reducing the stress to zero. During the time the rarefaction is propagating through the profile the free surface is accelerating

* 1 kbar = 10^9 dynes/cm^2 $\approx$ 1000 atm.

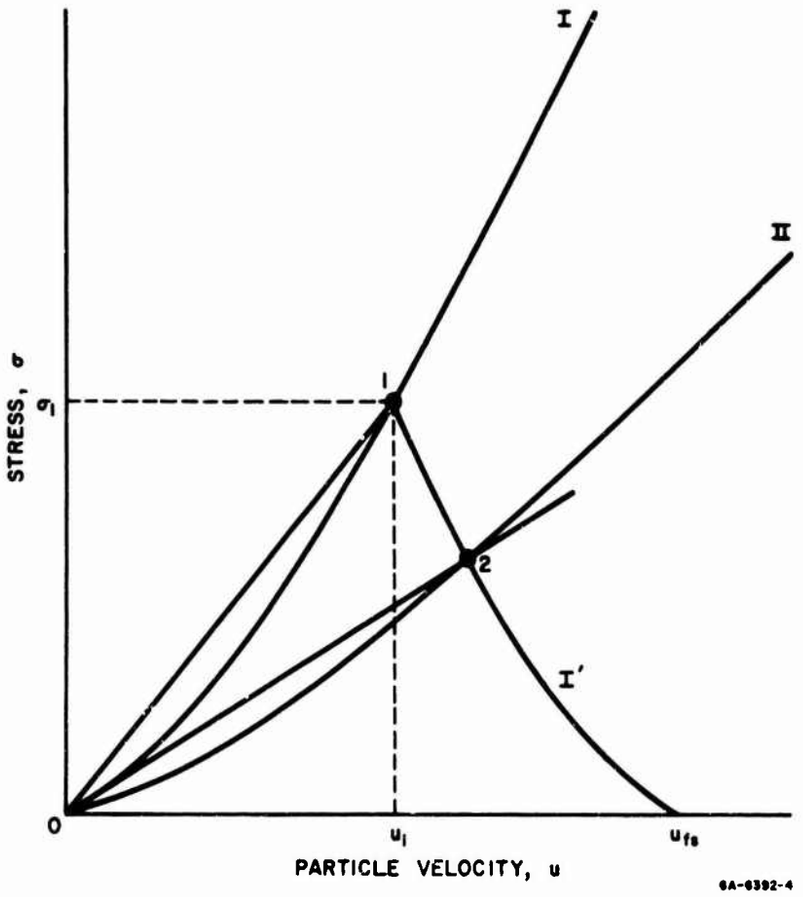

FIG. 4 HUGONIOTS AND RELEASE CROSS CURVE IN STRESS-PARTICLE VELOCITY PLANE

and the flow is quite complicated. After the rarefaction passes through the profile it reaches material which has been shocked to the final state σ_1, ρ_1, u_1. In materials in which the sound speed increases with compressive stress, compressive waves will steepen to form a steady-state shock. However, a sudden release of pressure, such as that occurring when the shock strikes a free surface, produces a rarefaction wave which flattens out or decreases the gradients as it propagates. Therefore rarefactions are treated as isentropic waves; in contrast, the entropy must increase through the shock zone. Referring to the stress-particle velocity diagram for material I in Fig. 4, the material at shock state 1

is released to zero stress isentropically down the curve I′, which is called a cross curve. In releasing the stress to zero, the rarefaction wave accelerates the material to a final velocity u_{fs} (free surface) at zero stress. If the incident shock had been a step discontinuity, the free surface itself would have moved off with this velocity instantaneously. Due to the profile, however, a finite time is required to accelerate the free surface to the velocity u_{fs}.

The curve I in Fig. 4 is a Hugoniot and the curve I′ is an isentrope. In cases where the entropy increase of the material due to the shock process is small, the Hugoniot curve may be treated approximately as an isentrope. In this approximation, the curves I and I′ are mirror images of one another about the line $u = u_1$. The free-surface velocity u_{fs} is then equal to $2u_1$, so that a measurement of the free-surface velocity is equivalent to a measurement of the particle velocity behind the shock. It must be emphasized that the approximation of $u_{fs} = 2u_1$ is based on assuming the shock process is reversible, and careful consideration must be given to each case in which it is applied.

If the shock in material I represented by state 1 in Fig. 4 were to arrive at an interface with material II, whose Hugoniot is given by curve II, the stress in material I would be altered. A shock would be transmitted into material II and the shock state would lie on curve II. A wave would be reflected back into material I. Since particle velocity and stress must be continuous across the interface the reflected wave in material I would be a rarefaction relieving the material to state 2, the point at which the release isentrope for material I intersects the Hugoniot of material II.

Impedance Match Technique for Measuring Hugoniots and Release Isentropes

If the equation of state relating stress, specific volume, and specific internal energy is known, it is possible to compute both the Hugoniot curve and the release cross curves in the stress-particle velocity plane. Extensive experimental shock wave work and calculations based on the Mie-Grüneisen equation of state have been performed on 2024 aluminum (Rice et al., 1958). The 2024 aluminum alloy has therefore been adopted

as a standard material, since its Hugoniot and release cross curves are well-known. Using this material it is possible to determine the Hugoniot of an unknown material by measuring the shock velocity through the unknown and the free-surface velocity of the standard material upon which the sample is mounted.

To perform the experiment the sample is mounted on a 2024 aluminum driver plate. A plane shock pulse of long duration is induced into the aluminum by impact from a high velocity metal plate or from the detonation of an explosive. Referring back to Fig. 4, let the curves I and II represent the aluminum and the sample material, respectively. In all cases studied the impedance of the sample material is lower than that of aluminum. The reflection at the interface of the initial shock in the aluminum then produces a rarefaction in the aluminum, relieving it from state 1 to state 2, and a shock in the sample that shocks it from state 0 to state 2. Measurement of the free-surface velocity of the aluminum locates the point u_{fs} and, since the cross curves for aluminum are known, this determines point 1, the state behind the initial shock in aluminum. Measurement of the shock velocity, U, through the sample is sufficient to determine the Rayleigh line 0-2 (see Fig. 4) of slope $\rho_o U$, where ρ_o is the initial density of the sample. The boundary condition of continuity of particle velocity and stress across the interface then requires that the Hugoniot point of the sample be state 2, the intersection of the cross curve of aluminum (I′) and the Rayleigh line of the sample. This technique, which is called the impedance match method, avoids having to rely on a measurement of the free-surface velocity of the sample to determine the particle velocity. In the case of shocks propagating in porous or highly compressible media, the assumption that the shock is isentropic is quite poor and measurement of the free-surface velocity does not yield the particle velocity. In such cases the impedance match technique must be used.

The impedance match technique can also be used to measure the cross curves of a material whose Hugoniot is already known. Suppose, in Fig. 4, the curve labeled I is the Hugoniot of the sample material and curve II is the known Hugoniot of another lower impedance material. A

shock is passed from the sample material (I) into the lower impedance material (II), which is called the buffer. As the shock passes from I to II a rarefaction is reflected back into I. This rarefaction relieves the stress adiabatically in I and increases the particle velocity. The stress-particle velocity states that material I pass through during this process lie on the cross curve that is being studied. Measurement of the shock velocities in the two materials yields the points 1 and 2. However, because of the continuity of particle velocity and stress across the interface, point 2 also must lie on the material I cross curve. By using several buffers with known Hugoniots, several points on the cross curve can be obtained. Measurement of the free-surface velocity yields the zero stress point on the cross curve. Thus the free-surface velocity is useful as a cross curve point.

EXPERIMENTS

Sample Materials

Hugoniot measurements were made on Ottawa banding sand of various saturations, West Lebanon glacial till of various saturations, and monocrystalline and fine-grained polycrystalline ice. Release curve measurements were made on dry and saturated Ottawa banding sand and on polycrystalline ice. The low-impedance buffer materials for release curve measurement on the sand were polycrystalline ice, Eccofoam SI,* and air. The buffers for ice were Eccofoam SI and air. The air buffer measurement is just a measurement of the free-surface velocity. Eccofoam SI is a polyester foam, containing silica microballoons, which has a density of 0.55 g/cm^3. In the course of the work it was necessary to measure the Hugoniot of the Eccofoam SI so that it could be used as a buffer.

Ottawa Sand. The coarse soil material studied was Ottawa banding sand obtained from the Ottawa Silica Company, Ottawa, Illinois. The grains of this silica sand are quite spherical and uniform in size. Prior to sample preparation the material was screened, and that portion which passed a No. 100 screen but failed to pass a No. 200 screen was used in testing. Particle sizes ranged from 74 to 149 microns. The sample material was washed to remove the very fine material which adheres to the grains and does not pass the No. 200 screen. The sand was then dried and stored in sealed bottles.

The dry porosity of all Ottawa banding sand samples was n = 0.372. The porosity, n, is defined as $n = 1 - (\rho_d/\rho_x)$; ρ_d = apparent dry density and ρ_x = crystal density. This porosity corresponds to a dry density of 1.65 g/cm^3. The crystal, or void-free, density was taken to be $\rho_x = 2.63$ g/cm^3, which is that of quartz. The four degrees of saturation

---

* Trademark of Emerson and Cummings, Inc., Canton, Massachusetts.

studied were 100%, 50%, 20%, and 0%. The specifications at room temperature were:

Specimen 1 (100%)		Specimen 2 (50%)	
ρ_d	= 1.65 g/cm^3	ρ_d	= 1.65 g/cm^3
ρ_t	= 2.02 g/cm^3	ρ_t	= 1.84 g/cm^3
ω	= 22.5%	ω	= 11.3%
S	= 100%	S	= 50%
n	= 0.372	n	= 0.372

Specimen 3 (20%)		Specimen 4 (0%)	
ρ_d	= 1.65 g/cm^3	ρ_d	= 1.65 g/cm^3
ρ_t	= 1.72 g/cm^3	ρ_t	= 1.65 g/cm^3
ω	= 4.5%	ω	= 0%
S	= 20%	S	= 0%
n	= 0.372	n	= 0.372

Here ρ_t is the total density (including water), ω is the percent water based on dry weight, and S is the percent saturation.

Upon freezing, the 100% saturated sand sample expanded because of the expansion of the water that filled the voids. Using a frozen water density of 0.917 g/cm^3 at -10°C and atmospheric pressure (Dorsey, 1940), the specifications of the saturated sample (Specimen 1 at -10°C) would be:

ρ_d	= 1.59 g/cm^3
ρ_t	= 1.96 g/cm^3
ω	= 22.5%
S	= 100%
n	= 0.395

West Lebanon Glacial Till. A sample of West Lebanon glacial till was received from USA CRREL. When the material was screened to obtain the particle size distribution, it was found that 99% was less than

149 μ, 72% was less than 74 μ, and 20% was less than 44 μ. The saturations of interest were 100%, 53%, and 0%. Specimens were prepared to conform to specifications set up by USA CRREL. The room-temperature dry porosity of all samples of the West Lebanon glacial till was n = 0.351. The room-temperature specifications were:

Specimen 1 (100%)		Specimen 2 (53%)	
ρ_d	= 1.86 g/cm^3	ρ_d	= 1.86 g/cm^3
ρ_t	= 2.21 g/cm^3	ρ_t	= 2.05 g/cm^3
ω	= 19.0%	ω	= 10%
S	= 100%	S	= 53%
n	= 0.351	n	= 0.351

Specimen 3 (0%)

ρ_d	= 1.86 g/cm^3
ρ_t	= 1.86 g/cm^3
ω	= 0%
S	= 0%
n	= 0.351

Again, due to the expansion upon freezing of the water filling the voids, the specifications of the saturated soil (Specimen 1 at -10°C) became:

ρ_d	= 1.80 g/cm^3
ρ_t	= 2.14 g/cm^3
ω	= 19%
S	= 100%
n	= 0.370

Ice. Monocrystalline and fine-grained polycrystalline ice samples were prepared by USA CRREL and sent to SRI in the form of disks, nominally 1 inch in diameter by 3/16-inch thick. The density of ice at -10°C and atmospheric pressure was taken to be 0.917 g/cm^3 (Dorsey, 1940).

Sample Preparation

All soil, ice, and foam samples used in the experiments were nominally 3/16 inch thick. The ice and soil samples used in the Hugoniot experiments were 1 inch in diameter whereas the same materials used in the release curve experiments were 1-3/4 inches in diameter. These sample diameters insured at least a 1/2 inch diameter central region of the sample which was free of edge effects for the duration of the experiment.

In the case of the Ottawa sand, the coarsest of the two soils studied, the sample thickness of 3/16 inch is about 30 times the diameter of the largest particles. It was felt that this ratio of sample thickness to particle size was sufficiently large so that the shock thickness could be considered small compared to the sample thickness. At lower stresses (stresses of the order of the crushing strength of the soil) a double elastic-plastic wave structure would be expected. In this case the plastic wave might have a long rise time and the effect of particle size on wave structure would have to be examined more closely.

The most convenient way to handle the soil samples was to prepare them in aluminum rings sandwiched between an aluminum base plate and a glass cover with a mirror coating on it. These mounting components are shown in Fig. 5. From left to right in the figure are the mirrored cover

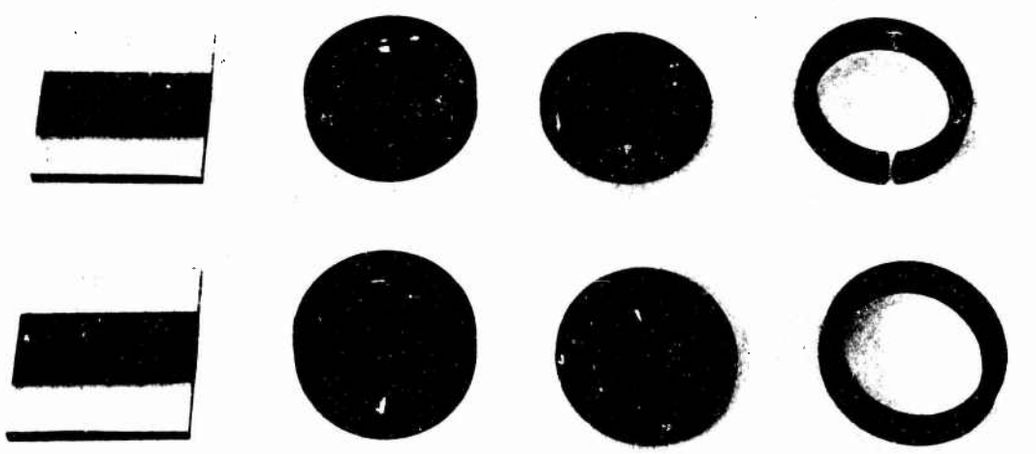

GP-6392-6

FIG. 5 SAMPLE RINGS

glasses, the rings mounted on the aluminum base plates, the base plates alone, and the rings alone. The upper assembly, containing the ring with a slot cut in it, was for the saturated samples. The slot provided a path for the material to expand upon freezing.

The aluminum was glued to the base plate with an epoxy cement. The unit was then weighed, the dimensions of the ring and base plate were measured, and the volume was computed. To prepare the dry sand samples a mass of dry sand was weighed out for each ring sufficient to fill the volume at a density of 1.65 g/cm^3. The ring was inserted in a jig (see Fig. 6). The sand was tapped and smoothed until it was nearly contained in the ring. The plunger was inserted and compaction to the final density of 1.65 g/cm^3 was performed in a press. The sample was then removed from the jig and reweighed, to be sure no material was lost. A 1-1/4-inch-square glass cover with a 1/2-inch mirror strip (see Fig. 5) was then cemented, mirror coating side down, on the ring with Eastman 910 cement. The samples were stored in a desiccator for eventual use. All sample densities were rechecked before they were used. If the densities were not 1.65 ± 0.01 g/cm^3, the samples were not acceptable.

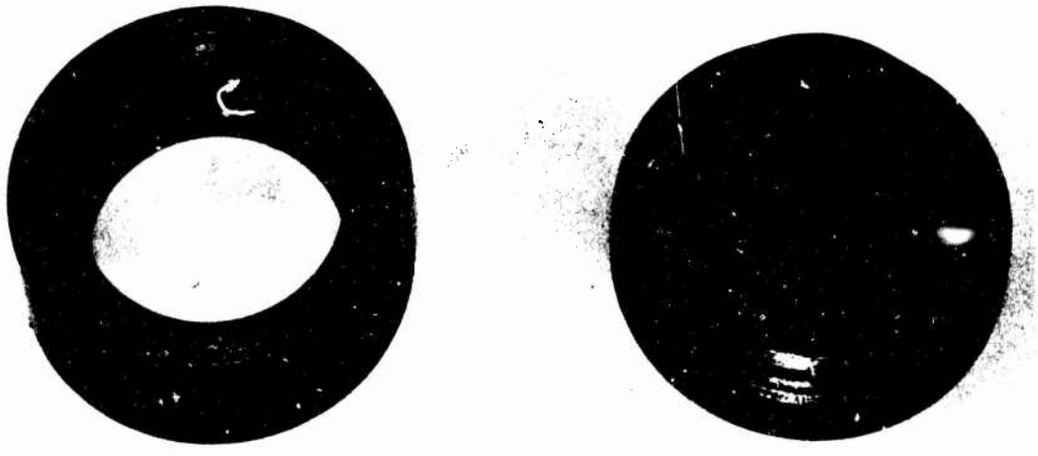

GP-6382-7

FIG. 6 LOADING JIG AND PLUNGER

The 100% saturated samples were prepared in the aluminum sample rings with a 1/16-inch slot milled through one side (see Fig. 5). These slots were initially filled with Silastic and the sample was prepared dry to a density of 1.65 g/cm^3 as described above. The Silastic plug was then removed and the sample was placed in a beaker under 1-1/2 inches of dry sand. The beaker was placed in a vacuum chamber and the pressure was reduced to about 50 mm Hg for one hour. The beaker was filled with degassed water while it was still at reduced pressure. The sample was then tapped to remove all trapped air bubbles. The vacuum was released and reestablished. After this treatment the sample was weighed and the density was computed to be sure the material was saturated. Acceptable samples were then placed in a freezer between two lapped plates in a clamp, as shown in Fig. 7. During freezing some sand and water extruded through the slot, due to expansion of the water. After freezing the sample density was rechecked.

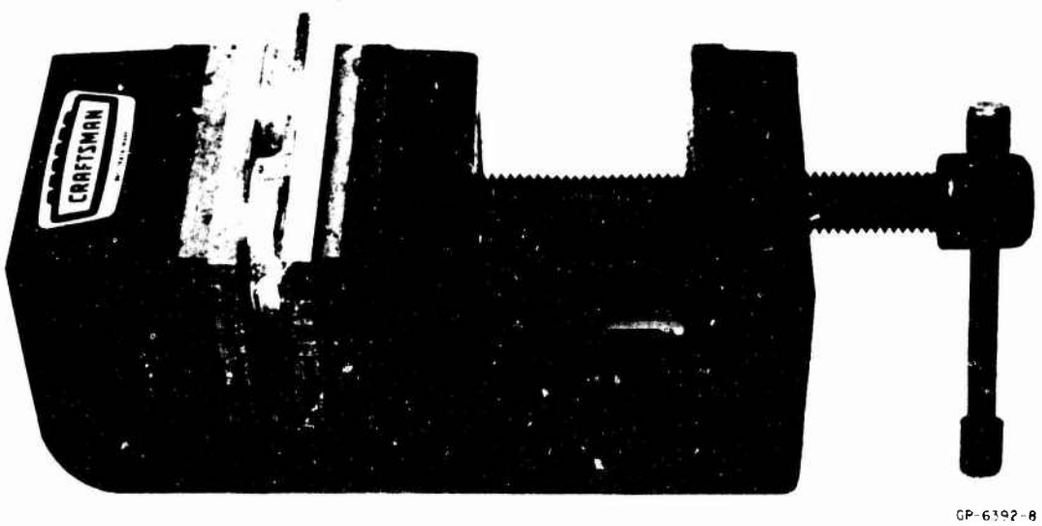

FIG. 7 FREEZING CLAMP

Partially saturated sand was prepared in bulk and stored in sealed jars. However, it was found that uniform moisture content could not be maintained in such large quantities. Consequently, an amount of partially

saturated sand just sufficient to fill one ring assembly was prepared at one time. This was done by thoroughly mixing a predetermined mass of sand and water, placing it in the ring, compacting with the press, and sealing with the mirror glass. The partially saturated samples were then sealed with an additional layer of Silastic and stored in a humid box to prevent moisture loss.

The West Lebanon glacial till samples were prepared in the same type of rings that were used for the Ottawa sand. The till compacted easily. The saturated samples were prepared in the grooved rings under reduced pressure with deaired water in the same manner as the saturated sand. The 53% saturated till was prepared from a master batch at a 10% water content. This large sample was stored in sealed jars, and the moisture content of random samples was checked before the material was used. If the moisture content fell outside the range 10% ± 0.3%, a new batch was prepared.

Checking of stored, frozen, saturated till samples revealed that the samples changed with age, apparently because of the migration of unfrozen water. Consequently, the saturated till samples were placed in the clamp assembly, quick-frozen with dry ice, and allowed to come up to -10°C. Quick freezing reduces water migration during the freezing process.

The ice samples, supplied by USA CRREL in disks 1 inch in diameter and from 3/16 inch to 1/4 inch in thickness, were mounted in aluminum sample rings. The rings were glued to the mirror and chilled down to slightly above 0°C. The unit was then placed, mirror down, on an aluminum block in a freezer held at -15°C. The ice was placed in the ring and a weight was placed on the back of the ice. Heat transfer from the ring to the ice caused melting in a very thin layer of ice adjacent to the ring, which brought the ice into close contact with the mirror surface. The small amount of water produced by the melting quickly refroze. The back surface of the ice was shaved off flush with the ring by using

a cold glass blade at an angle of about 20°. After shaving the sample was measured with a cold micrometer; if it was uniform to within 0.001 inch, a cold aluminum base plate was attached.

The ice and sand samples used in the experiments to measure release cross curves were prepared in an aluminum ring with a base plate in a manner similar to that used in preparing the Hugoniot samples. However, the samples were covered with a thin (0.0007-inch) layer of aluminized Mylar instead of a mirrored cover glass. Aluminized Mylar was used to act as a mirror and form a thin membrane to separate sample and buffer. The buffer material, either ice or Eccofoam SI, was placed in another aluminum ring over the Mylar-covered sample, and a cover glass with a mirrored strip was placed over the buffer material. The ice and sand samples used for free-surface velocity measurements were prepared in an aluminum ring and were then covered with a thin metal shim. An inclined free-surface velocity mirror was mounted on the shim.

Experimental Procedures

All plane shock waves were produced either by the impact of an explosively accelerated flat metal plate or by the detonation of an explosive pad in contact with the test assembly. The flying plate assembly is shown schematically in Fig. 8. The plane wave explosive lens induced a plane detonation wave into an 8-inch-diameter cylindrical pad of explosive. The detonation wave propagated through the explosive and the detonation products accelerated a metal plate across an air gap. The thickness of the explosive pad and the type of explosive determined the final velocity of the flyer plate. The flyer plate struck, and induced a shock wave into, a 2024 aluminum driver plate upon which the samples were mounted. The flyer plate was sufficiently thick that, for the duration of the experiment, it could be considered semi-infinite.

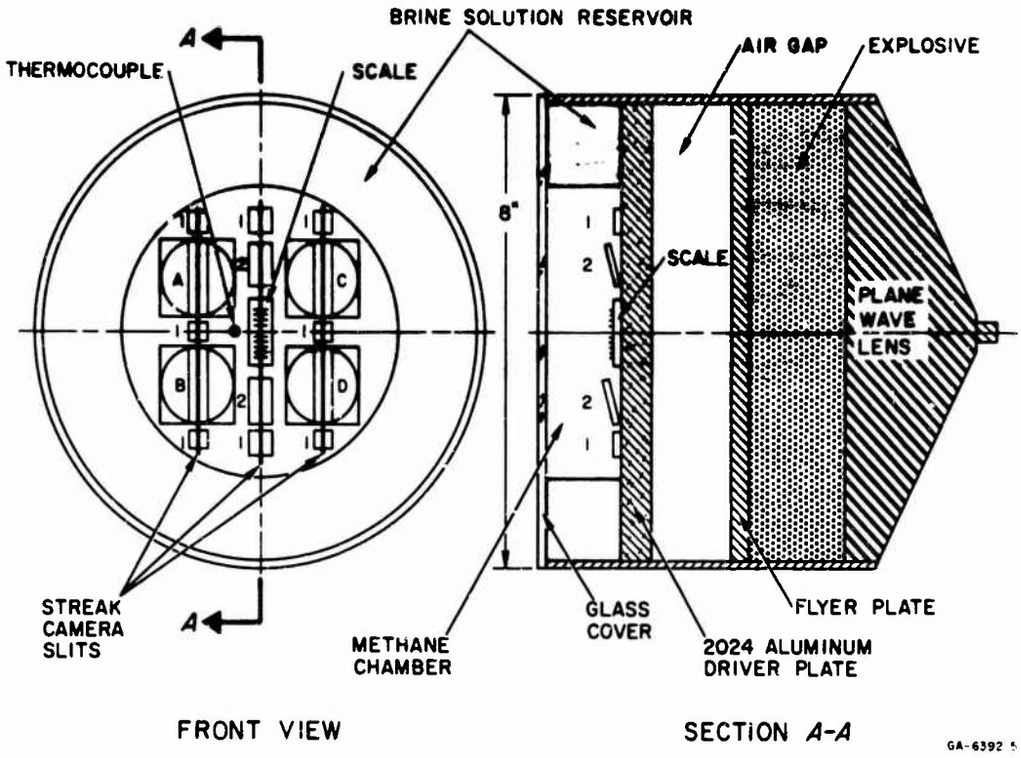

FIG. 8 FLYING PLATE DRIVER SYSTEM FOR STUDYING FROZEN MATERIALS

To determine Hugoniot points for the samples using the impedance match technique, the shock velocity through the sample and the free-surface velocity of the aluminum driver plate were measured. These measurements were made optically, using a Beckman and Whitley Model 770 rotating mirror streak camera. Four samples were placed on a shot and the face of the shot was observed through three slits of the streak camera. Small mirrors were mounted on the face of the shot and illuminated by an explosive light source. Referring to Fig. 8, the small mirrors labeled 1 were placed flat on the surface of the 2024 aluminum driver plate. They ceased to reflect light when they were destroyed by the shock breaking out of the aluminum; this cessation denoted the arrival time of the shock at the sample-aluminum interface. Mirrors A, B, C, and D are the glass covers placed over the sample rings. The destruction of these mirrors denoted the time of arrival of the shock at the

sample surface. The transit time through the sample could therefore be computed. It was assumed that a steady state is established in a time which is small compared to the total shock transit time through the sample. Therefore the shock velocity is simply the sample thickness divided by the transit time. This assumption of constant shock velocity becomes invalid if the rarefaction from the back of the flyer plate overtakes and attenuates the shock in the sample.

The free-surface velocity of the 2024 aluminum driver plate was measured by two inclined mirrors (labeled 2 in Fig. 8) mounted on the free surface. These were observed through the center of the three slits. Referring to the side view in Fig. 8, which shows the inclined mirrors, as the free surface moved out it progressively destroyed the inclined mirrors, producing an angular cutoff of reflected light reaching the film in the streak camera. Measurement of the cutoff angle on the film, together with knowledge of the initial angle of inclination of the mirrors on the free surface, the writing speed of the streak camera, and the shot-to-film magnification, was sufficient to compute the free-surface velocity. Flat mirrors (labeled 1) were mounted adjacent to the inclined mirrors to indicate shock tilt and curvature, which were taken into account in the film analysis.

The samples were maintained at $-10^{\circ}C$ by a chamber attached to the aluminum driver plate, which contained a $-10^{\circ}C$ melting brine solution. Temperature was monitored by a continuous-recording thermocouple mounted in the center of the shot. The temperature was always $-10 \pm 2^{\circ}C$. A glass plate was placed over the face of the shot and the region in front of the mirrors was flooded with methane to eliminate moisture condensation on the mirrors.

Photographs of the shot assembly are shown in Figs. 9 and 10. A typical streak camera record is shown in Fig. 11; in the left slit, the cutoffs of mirrors 1 are noted, indicating the arrival of the shock at the free surface. Cutoffs A and B are the shock breaking out of the sample. In the center slit, the cutoffs of the inclined mirrors are noted.

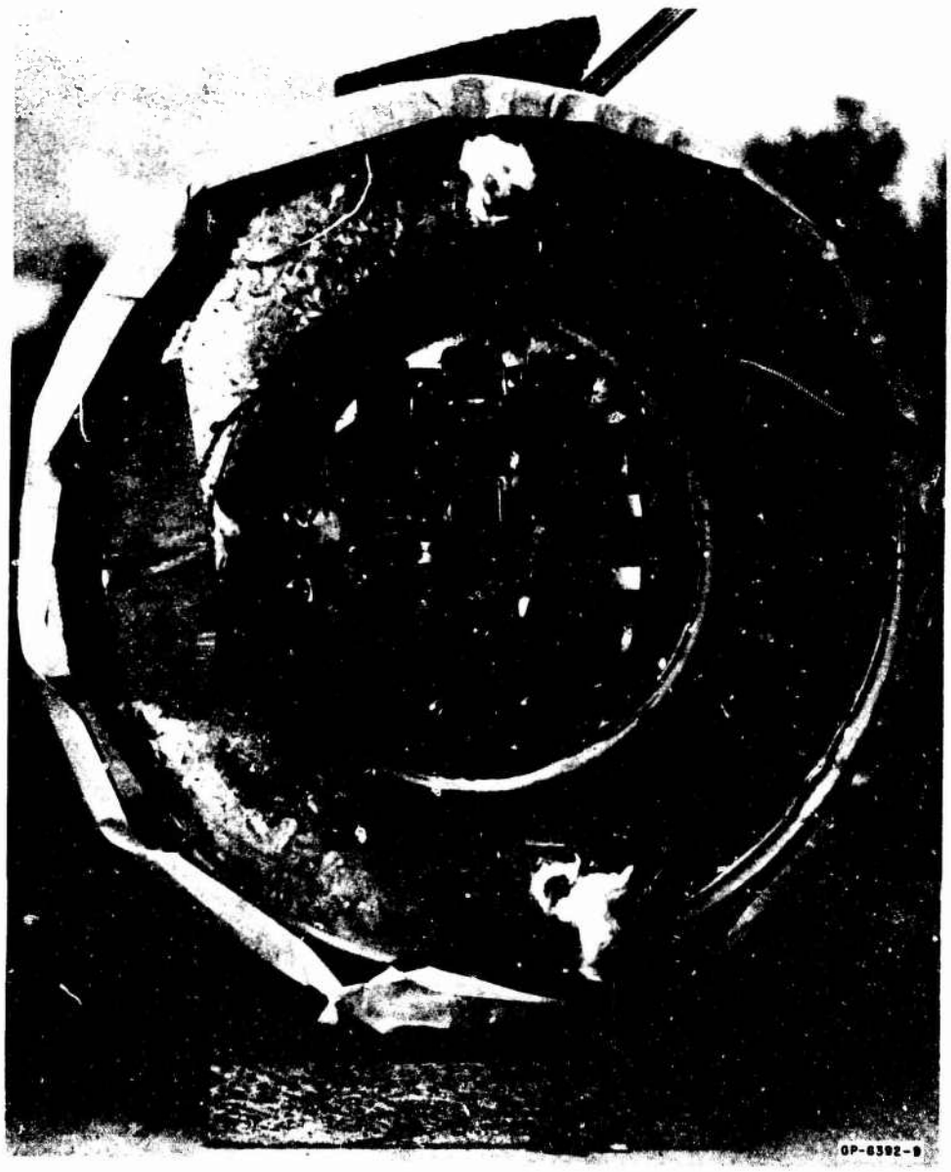

FIG. 9 FACE OF EXPLOSIVE ASSEMBLY

From the measured shock velocity through the sample and the free-surface velocity of the aluminum driver, the state behind the shock in the sample was computed, using the impedance match technique discussed in the previous section.

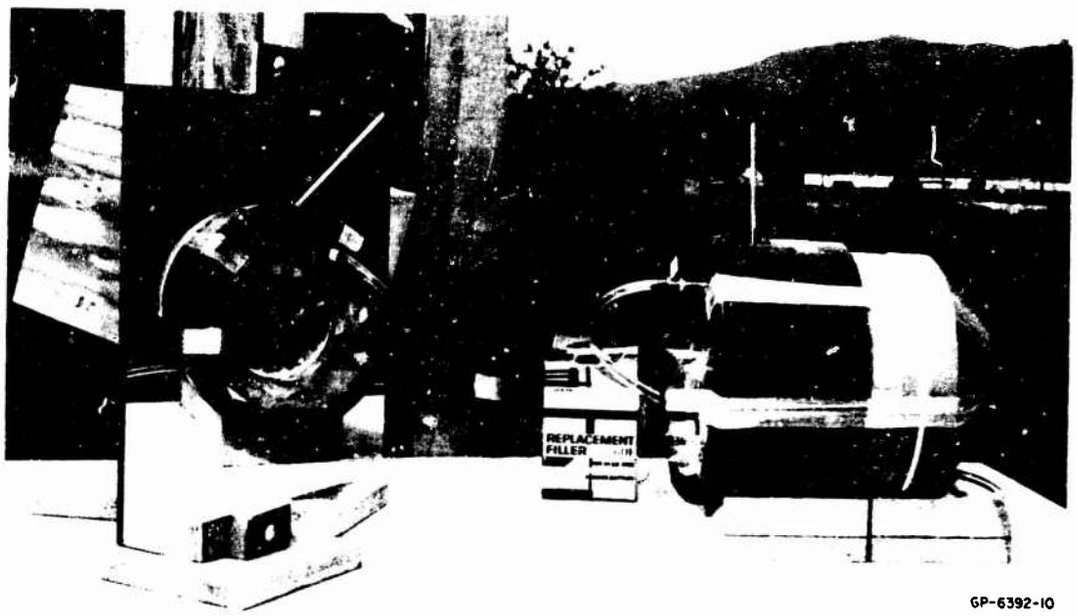

FIG. 10 FLYING PLATE EXPLOSIVE ASSEMBLY

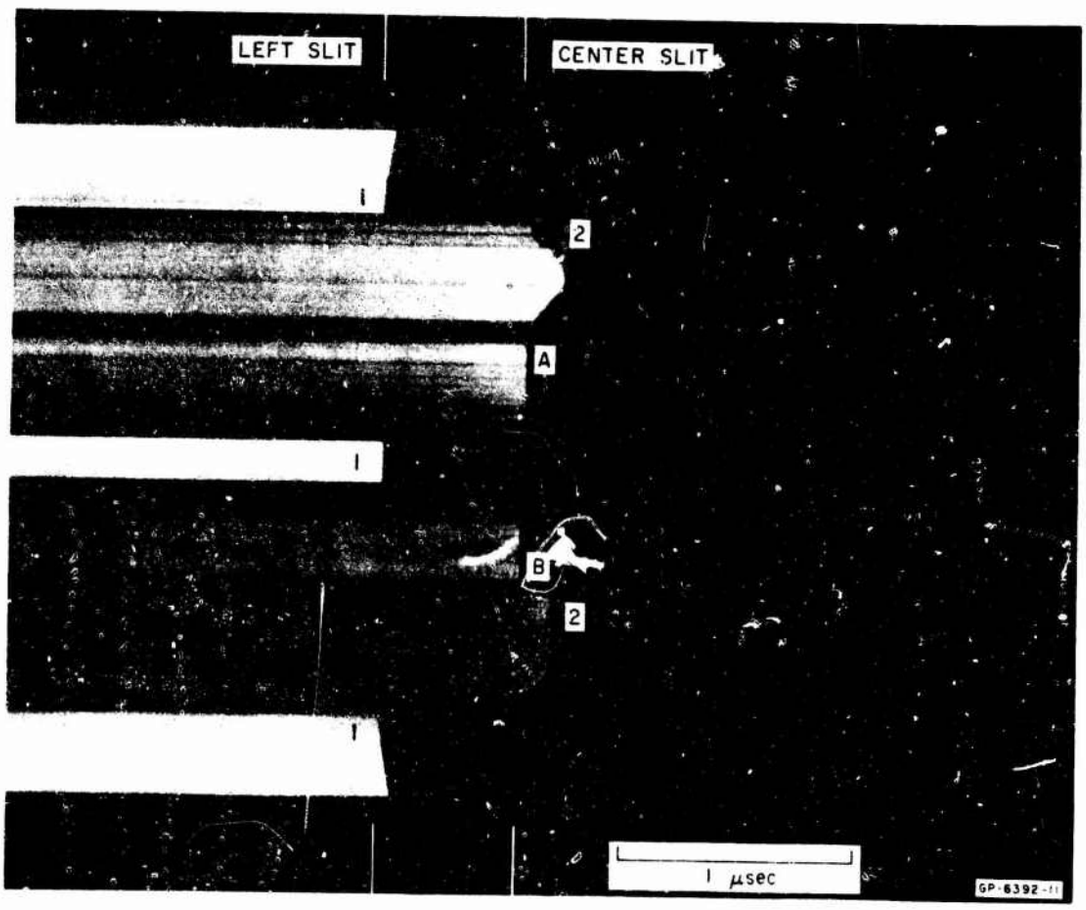

FIG. 11 STREAK CAMERA RECORD

The construction of the shot assemblies for measuring the release cross curves of ice and sand was quite similar to that for the assembly shown in Fig. 8. Only three samples were placed on each shot, since the additional thickness of the sample-buffer combination required a larger diameter sample to prevent edge effects from interfering with th. measurements. The arrival of the shock at the aluminum-sample interface was recorded by a set of small flat mirrors like the mirrors labeled 1 in Fig. 8. In the case of the ice buffer on top of the sand, the arrival of the shock at the sample-ice interface was recorded by the aluminized Mylar, which was observed through a portion of the transparent ice. The arrival of the shock at the ice free surface was recorded by the glass mirror, which covered a portion of the ice. The Eccofoam SI buffers did not completely cover the sand or ice samples upon which they were mounted, so the arrival of the shock at the sample-foam interface was again recorded by the aluminized Mylar that covered the sample. The arrival of the shock at the foam surface was recorded by a glass mirror. Inclined mirrors were used to measure free-surface velocities of both the samples and the aluminum driver plate.

In the cases of saturated and dry Ottawa sand, the shots were constructed so that three points were obtained on the same cross curve. Three samples were mounted on each assembly. One sample was covered by an ice buffer, one sample was covered by an Eccofoam SI buffer, and the third sample had an inclined mirror for free-surface velocity. Thus, all three samples were shocked to the same Hugoniot state but each was relieved to a different point on the same cross curve. In the case of the ice samples, only two points were obtained on each cross curve. One ice sample was covered by an Eccofoam SI buffer and the other had a free-surface velocity mirror on it. Since only two ice samples were mounted on each shot, the remaining space on the ice shots was used to mount an Eccofoam SI sample for the purpose of measuring its Hugoniot.

EXPERIMENTAL DATA AND RESULTS

Ottawa Sand

The Hugoniot data for the Ottawa banding sand are presented in Table I. The data are plotted in the stress-particle velocity, shock velocity-particle velocity, and stress-specific volume planes in Figs. 12, 13, and 14. The curves drawn through the points in these figures do not represent any type of fit, but are drawn simply as guides. The curves in the U - u plane (Fig. 13) exhibit a break, so a single straight line cannot be drawn through all the data. A dashed line has been inserted to indicate the region where the structure of the Hugoniot curve is not well defined. This change in the behavior of the Hugoniot is exhibited by an abrupt change in slope in the σ - V plane (Fig. 14) at about 280 kbar. This behavior is characteristic of quartz and is caused by the quartz-stishovite polymorphic phase transition (Ahrens et al., 1966).

West Lebanon Glacial Till

The Hugoniot data for West Lebanon glacial till are presented in Table II. The data are plotted in the σ - u, U - u, and σ - V planes in Figs. 15, 16, and 17. As in the case of Ottawa sand there is a steepening of the σ - V data (Fig. 17) at about 300 kbar, but it is not as well defined as in the case of the sand. This change in slope is reflected in Fig. 16 as a break in the U - u curve. This behavior is probably due to the quartz-stishovite phase change. The glacial till and banding sand data agree quite closely, especially at the high stress levels.

Table I

HUGONIOT DATA FOR OTTAWA SAND
(Initial Temperature = -10°C)

Shot Number	Sample Number	Shock Velocity (mm/μsec)	Particle Velocity (mm/μsec)	Stress (kbar)	Final Volume (cm^3/g)
Dry Sand, ρ_o = 1.65 g/cm^3					
12,930	S77	4.07	2.17	146	0.2823
12,929	S75	4.05	2.25	150	0.2697
12,908	S52	5.31	3.13	274	0.2486
12,928	S60	6.39	3.81	404	0.2449
Wet Sand, Saturation 20%, ρ_o = 1.72 g/cm^3					
12,907	S36	2.98	1.14	58	0.3590
12,942	S131	4.34	2.05	155	0.3071
12,930	S141	4.24	2.12	156	0.2906
12,940	S140	5.39	3.04	282	0.2527
12,916	S81	5.99	3.49	362	0.2428
12,941	S27	6.43	3.74	413	0.2431
Wet Sand, Saturation 50%, ρ_o = 1.84 g/cm^3					
12,931	S133	3.40	1.11	69.5	0.3661
12,942	S76	4.66	1.98	170	0.3127
12,933	S70	5.32	2.79	273	0.2584
12,940	S83	5.73	3.08	325	0.2509
12,932	S73	6.37	3.44	403	0.2499
Wet Sand, Saturation 100%, ρ_o = 1.96 g/cm^3					
12,907	S9	3.77	1.03	76	0.3708
12,947	S100-2	4.00	1.01	80	0.3813
12,931	S95	3.86	1.05	80	0.3714
12,929	S99	5.10	2.01	201	0.3091
12,933	S98	5.77	2.67	303	0.2736
12,915	S8	5.63	2.71	300	0.2646
12,908	S11	5.96	2.85	339	0.2632
12,916	S100-1	6.74	3.24	429	0.2649
12,932	S84	6.77	3.31	440	0.2603
12,928	S96	7.04	3.52	487	0.2550

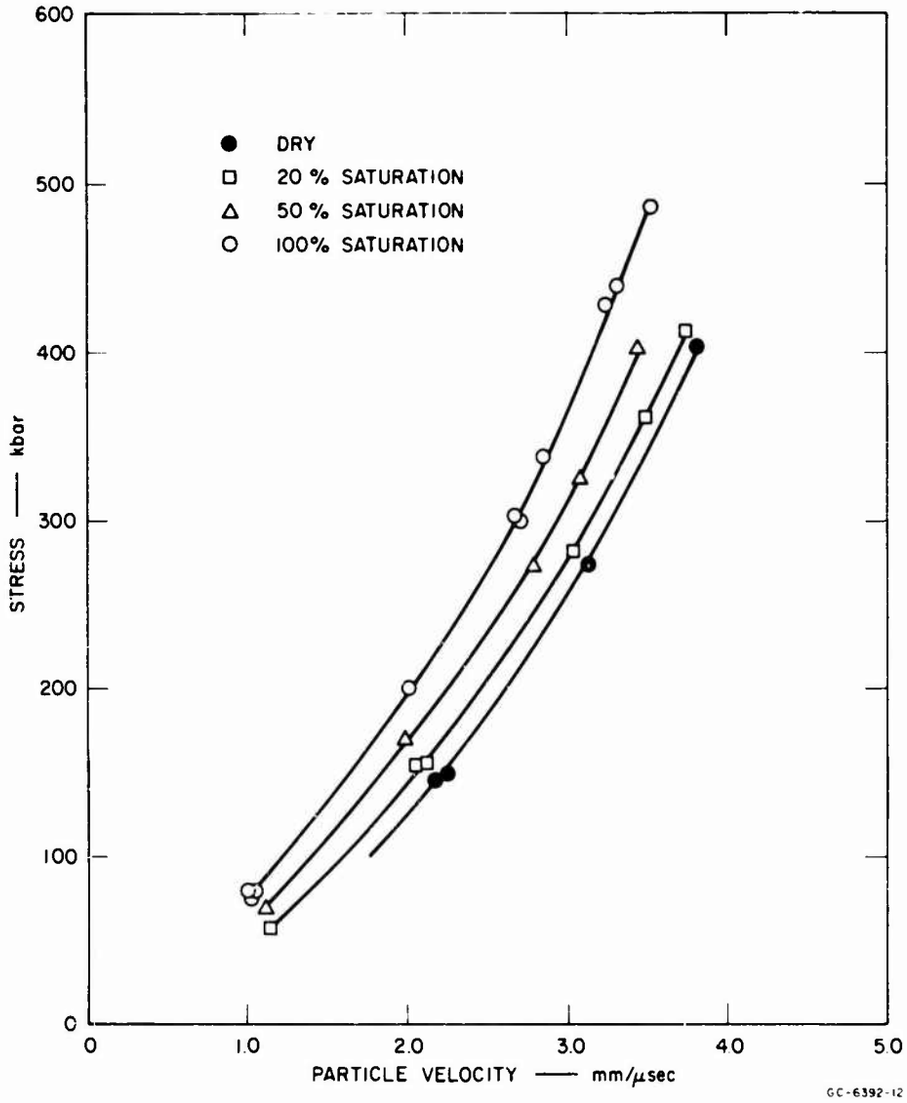

FIG. 12 HUGONIOT DATA FOR OTTAWA BANDING SAND (σ – u)

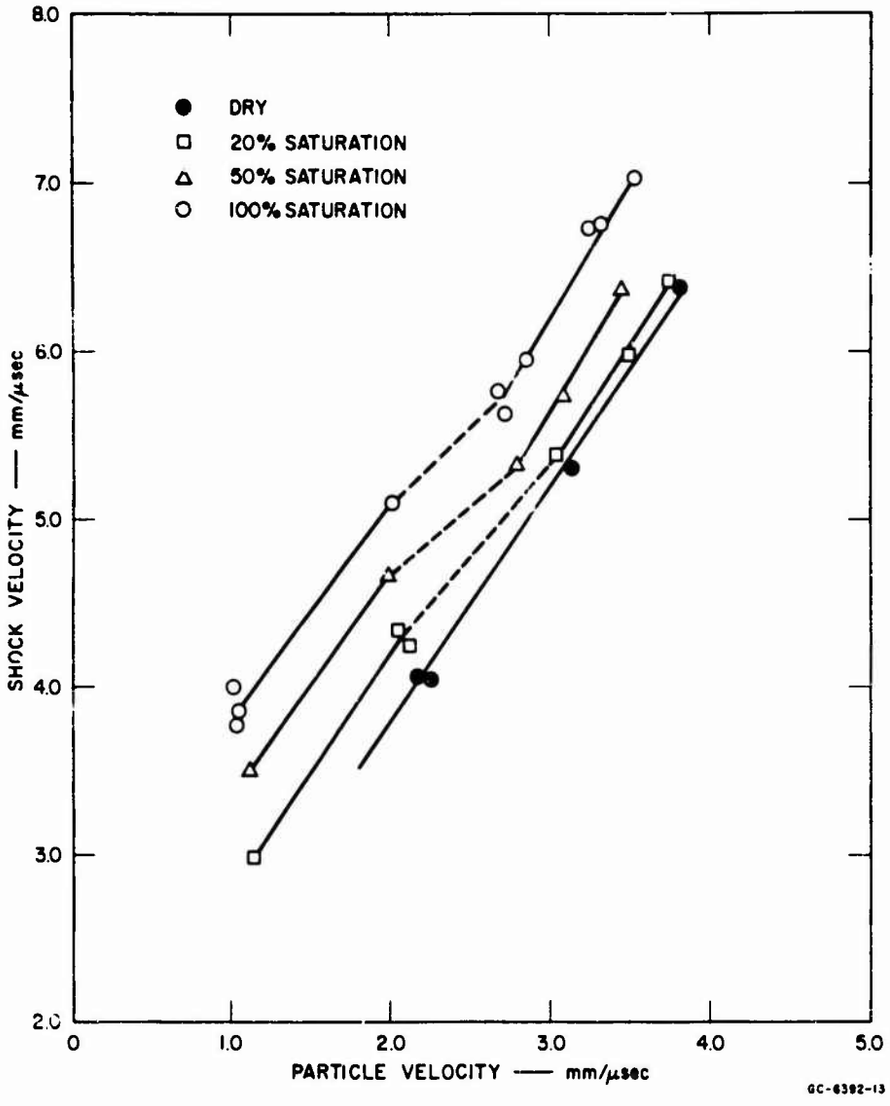

FIG. 13 HUGONIOT DATA FOR OTTAWA BANDING SAND (U – u)

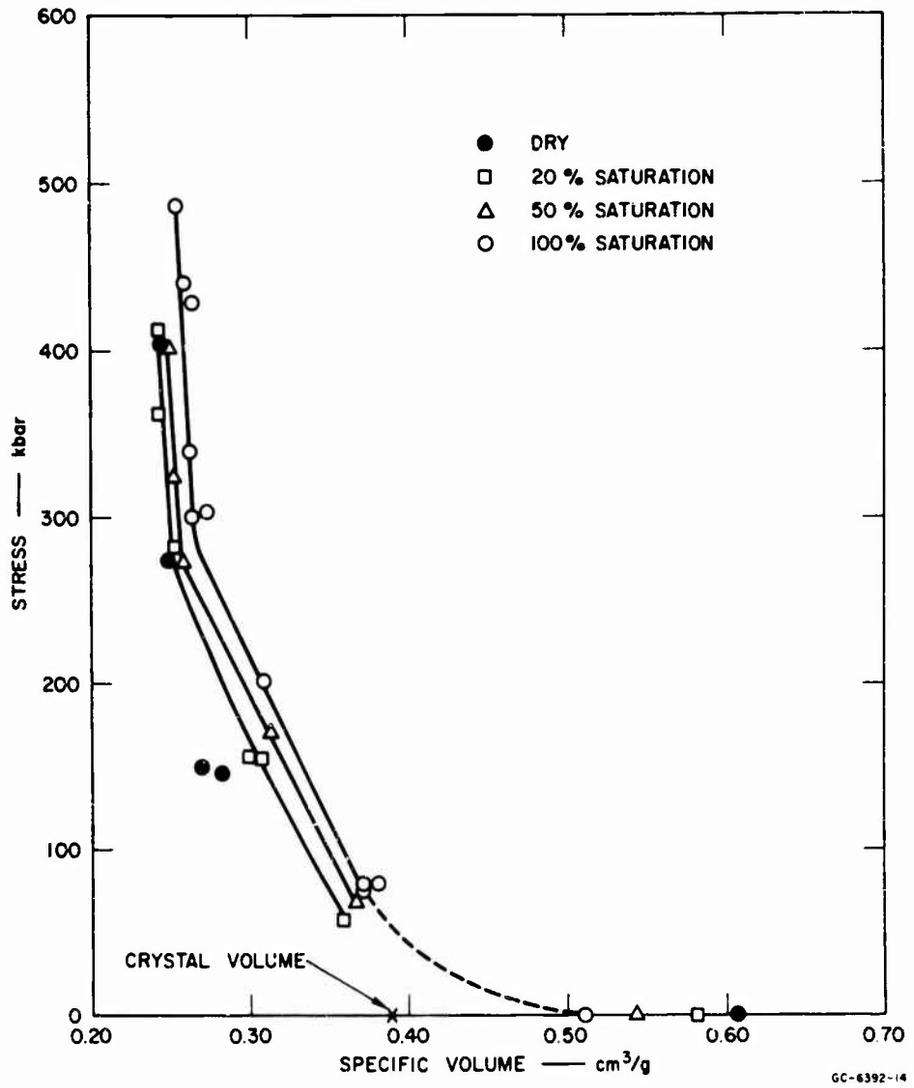

FIG. 14 HUGONIOT DATA FOR OTTAWA BANDING SAND (σ - V)

Table II

HUGONIOT DATA FOR WEST LEBANON GLACIAL TILL
(Initial Temperature = -10°C)

Shot Number	Sample Number	Shock Velocity (mm/μsec)	Particle Velocity (mm/μsec)	Stress (kbar)	Final Volume (cm^3/g)
Dry Till, ρ_o = 1.86 g/cm^3					
12,930	T65	4.19	2.08	164	0.2695
12,929	T51	4.17	2.16	167	0.2589
12,940	T19	5.62	2.94	308	0.2552
12,928	T63	6.57	3.65	451	0.2393
Wet Till, Saturation = 53% ρ_o = 2.05 g/cm^3					
12,907	T58	3.59	1.03	76	0.3470
12,931	T79	3.52	1.07	77	0.3397
12,942	T56	4.82	1.90	187	0.2958
12,930	T74	4.72	1.96	191	0.2853
12,933	T139	5.70	2.65	309	0.2610
12,915	T80	5.91	2.33	319	0.2703
12,908	T69	6.05	2.82	354	0.2593
12,916	T80	6.77	3.19	445	0.2581
12,932	T57	6.58	3.29	444	0.2440
12,941	T147	7.07	3.45	499	0.2500
Wet Till, Saturation = 100%, ρ_o = 2.145 g/cm^3					
12,907	T17	3.90	1.00	83	0.3466
12,929	T109	5.25	1.94	218	0.2939
12,915	T10-1	5.96	2.59	332	0.2636
12,916	T10-2	7.01	3.11	467	0.2593
12,928	T87	7.54	3.34	542	0.2596

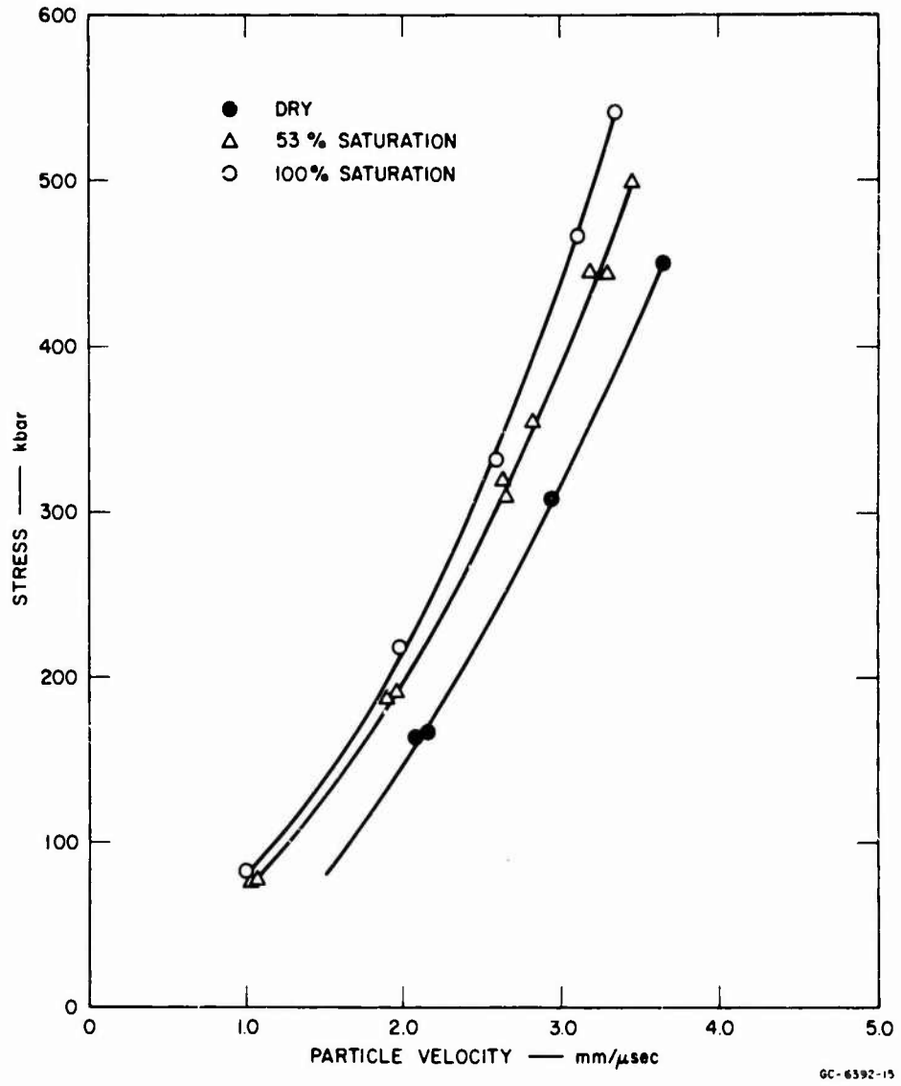

FIG. 15 HUGONIOT DATA FOR WEST LEBANON GLACIAL TILL (σ - u)

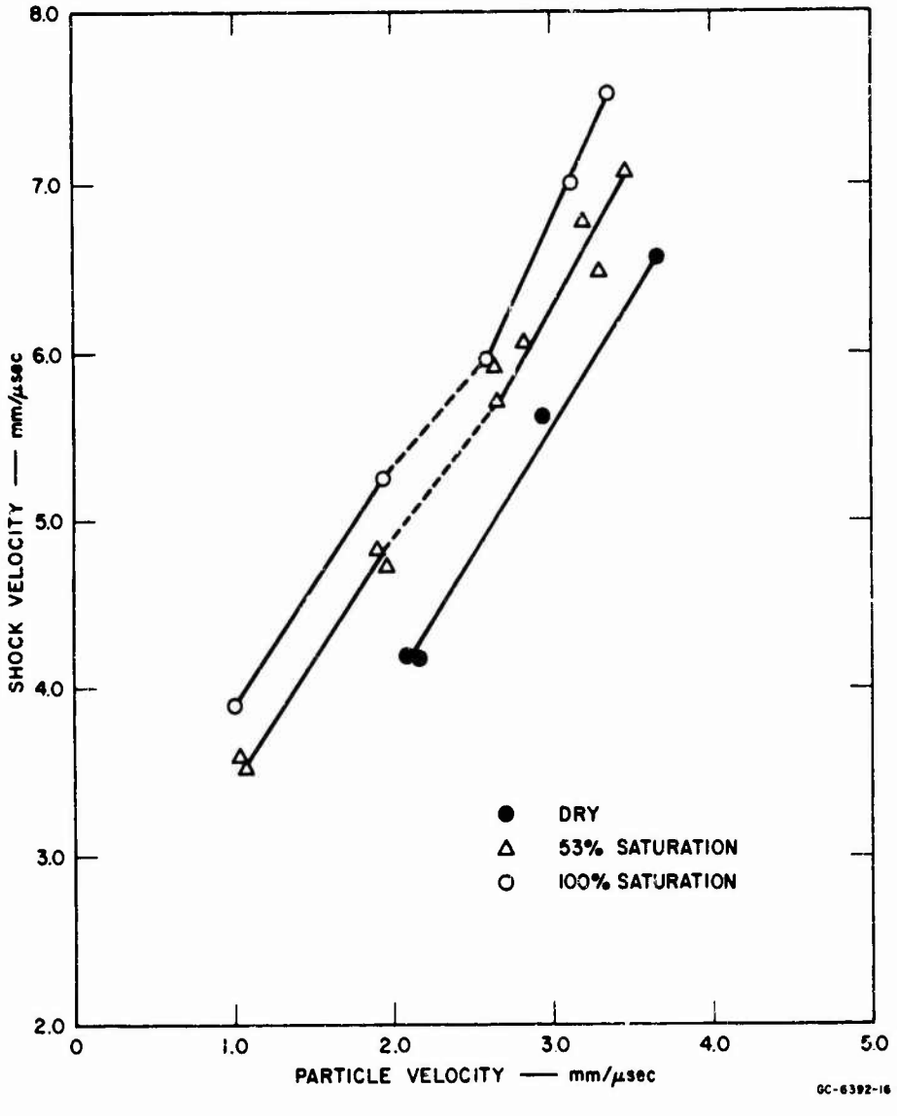

FIG. 16 HUGONIOT DATA FOR WEST LEBANON GLACIAL TILL (U – u)

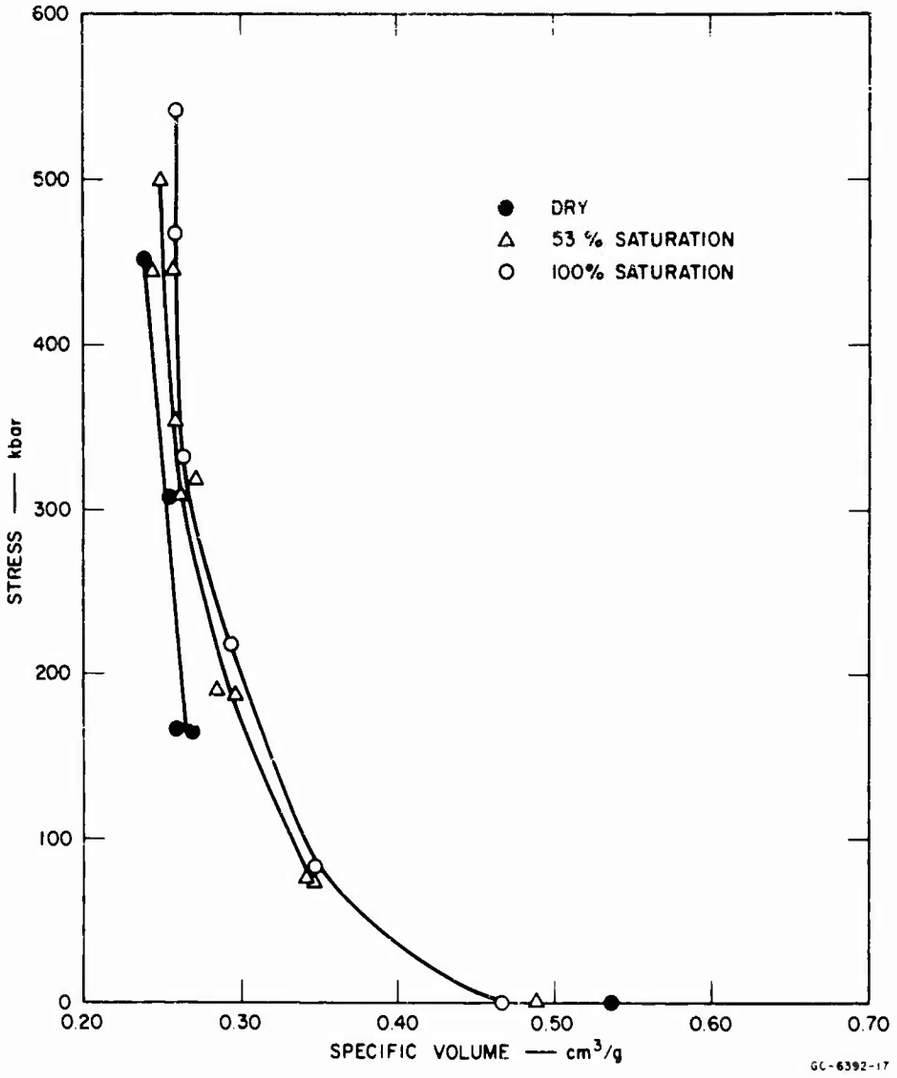

FIG. 17 HUGONIOT DATA FOR WEST LEBANON GLACIAL TILL (σ – V)

Ice

The Hugoniot data for ice are presented in Table III and Figs. 18, 19, and 20. Analysis of these data revealed no significant difference in the high pressure (stress) behavior of single and polycrystalline ice. The stress levels studied here were so high that no multiple wave structure arising from phase transitions of the type ice I - ice III, ice III - ice V, etc. would be expected.

Table III

HUGONIOT DATA FOR ICE
(Initial Temperature = $-10^{\circ}C$; $\rho_o = 0.917\ g/cm^3$)

Shot Number	Sample Number	Shock Velocity (mm/μsec)	Particle Velocity (mm/μsec)	Stress (kbar)	Final Volume (cm^3/g)
Monocrystalline Ice					
12,931	M3	2.95	1.30	35.5	0.6081[a]
12,947	M10	3.21	1.25	37.5	0.666
12,933	M4	6.12	3.19	180	0.5212
12,932	M7	7.55	3.94	274	0.5207
Polycrystalline Ice					
12,947	P7	3.23	1.25	37.5	0.6687
12,942	P2	5.00	2.30	106	0.5889
12,940	P3	6.72	3.36	207	0.5445
12,941	P1	7.81	4.19	301	0.5055

[a] This point is questionable because the shot record was poor.

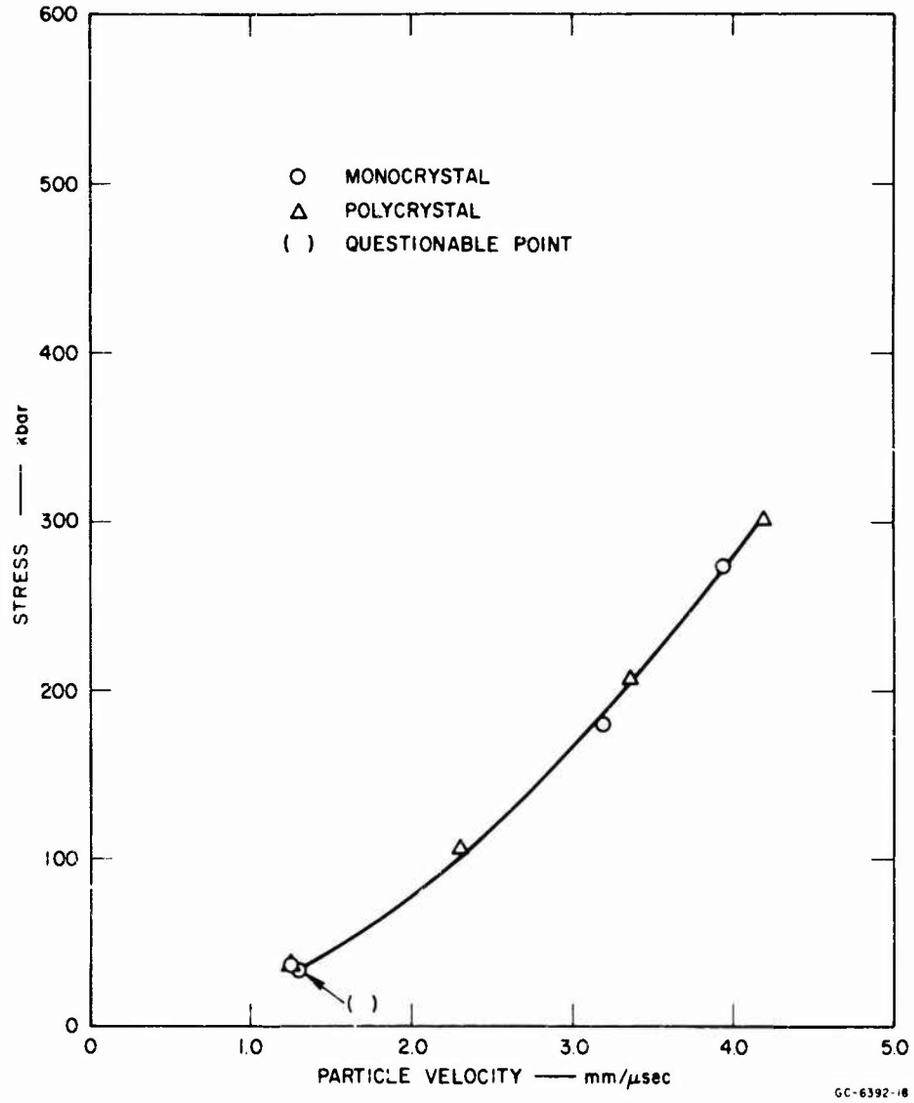

FIG. 18 HUGONIOT DATA FOR ICE (σ - u)

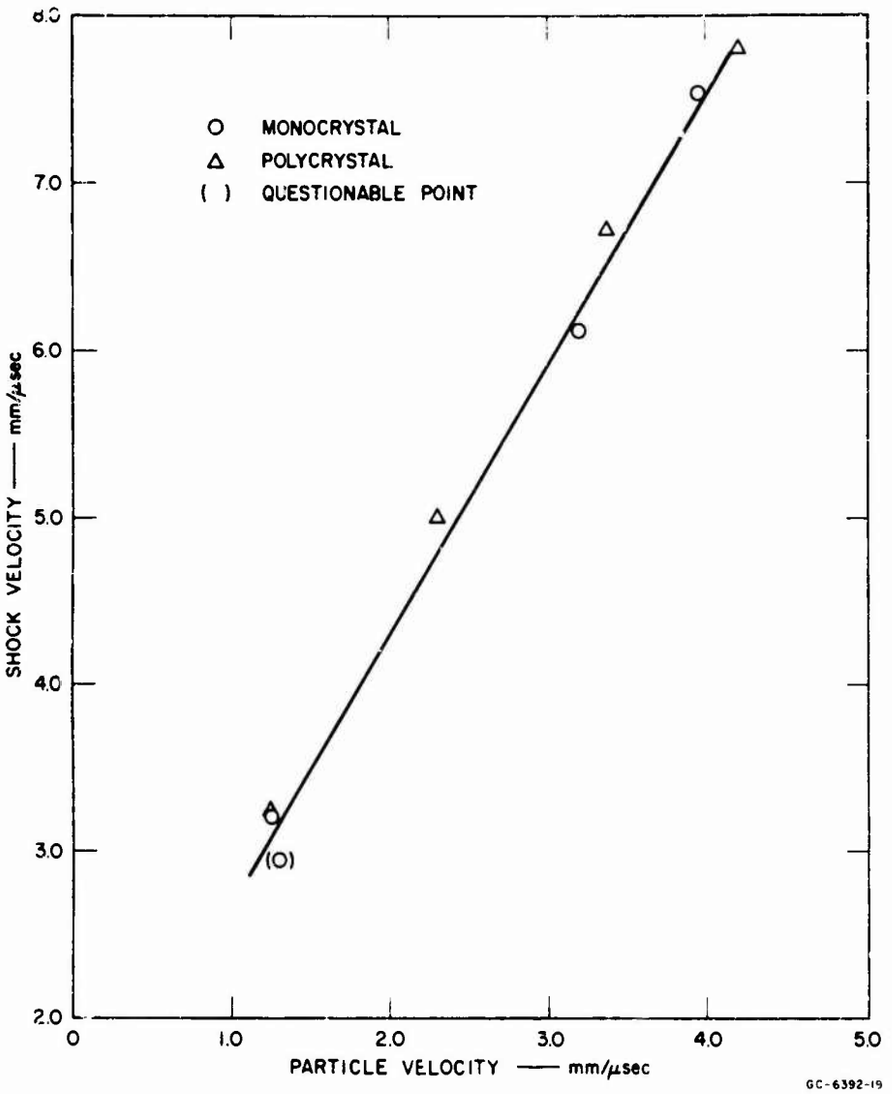

FIG. 19 HUGONIOT DATA FOR ICE (U - u)

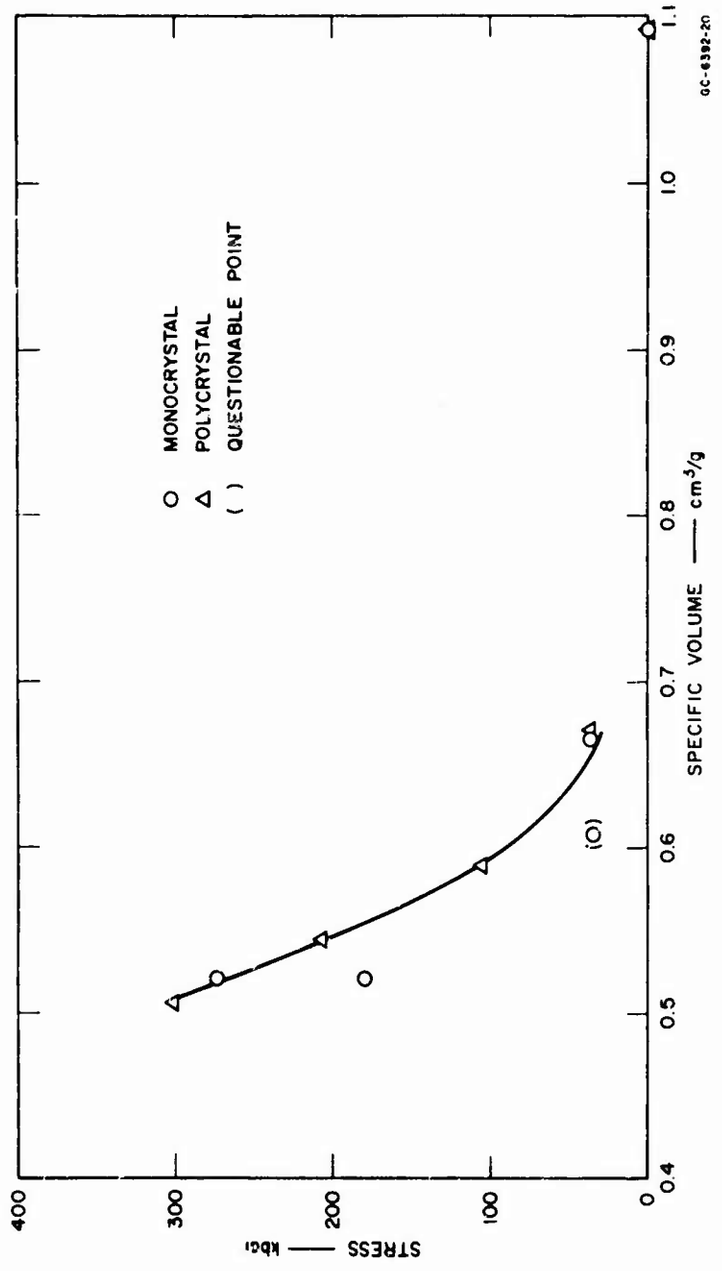

FIG. 20 HUGONIOT DATA FOR ICE (σ - V)

Release Cross Curves

A major problem in experiments to obtain release cross curve data on materials is that of maintaining a constant stress of sufficiently long duration on the driver plate that the shock can propagate through the driver, sample, and buffer material before being overtaken by the rarefaction from the back of the flyer plate. An obvious solution is to use a very thick flyer plate. This solution is satisfactory if low-velocity flyer plates are desired. However, there is a strong tradeoff between flyer plate thickness and the maximum velocity to which the plate may be accelerated by a given amount of explosive. The problem of attenuation of the shock wave by its being overtaken by the rarefaction is most serious in high stress experiments, i.e., experiments requiring high-velocity flyer plates. The explosive flyer plate system used to obtain release cross curve data from the highest stress Hugoniot state in the present study was therefore slightly different from the high velocity system used in the Hugoniot experiments. To accurately predict whether attenuation will occur requires knowledge of the longitudinal sound speed as a function of stress in aluminum, crushed sand, and crushed foam. Calculations using high estimates for these sound speeds (i.e., the worst possible case) indicate that the rarefaction would not be expected to overtake the shock until it had passed through at least two-thirds of the buffer. It was felt that the use of thinner buffers would decrease the precision of the experiments more than the amount of error introduced by a small amount of attenuation. No appreciable shock attenuation would be expected in the lower stress experiments.

The release cross curve data for Ottawa sand and polycrystalline ice are presented in Tables IV, V, and VI, and the data are presented graphically in the stress-particle velocity plane in Figs. 21, 22, and 23. These graphs also contain all the Hugoniot data for these materials. As in the previous graphs, the curves drawn do not represent any analytical fit to the data.

Table IV

RELEASE ADIABAT DATA FOR DRY OTTAWA SAND

(Initial Density = 1.65 g/cm^3)

Shot No.	Sample Thickness (mm)	Hugoniot State			Release Adiabat States			
		Shock Velocity (mm/μsec)	Particle Velocity (mm/μsec)	Stress (kbar)	Buffer Material	Particle Velocity (mm/μsec)	Stress (kbar)	Shock Velocity in Buffer (mm/μsec)
13,096	4.572	4.00	2.07	137	ice	2.30	103	4.89
	4.572	4.15	2.06	141	foam	2.57	44.3	3.13
	4.610[a]	--	--	--	air[b]	2.92	0	--
13,095	4.572	5.34	3.10	273	ice	3.44	213	6.75
	4.572	5.19	3.12	267	foam	3.96	108	4.98
	4.587[a]	--	--	--	air[b]	5.17	0	--
13,137	4.572	6.05	3.53	352	ice	3.78	253	7.30
	4.567	6.14	3.51	356	foam	4.17	121	5.26
	4.607[a]	--	--	--	air[b]	6.34	0	--

a. Only free-surface velocity was measured on this sample.
b. Buffer was air, so particle velocity corresponds to free-surface velocity.

Table V

RELEASE ADIABAT DATA FOR SATURATED OTTAWA SAND

(Initial Density = 1.96 g/cm^3)

Shot No.	Sample Thickness (mm)	Hugoniot State			Release Adiabat States			
		Shock Velocity (mm/μsec)	Particle Velocity (mm/μsec)	Stress (kbar)	Buffer Material	Particle Velocity (mm/μsec)	Stress (kbar)	Shock Velocity in Buffer (mm/μsec)
13,092	4.597	5.20	1.83	187	ice	2.41	112	5.06
	4.597	5.19	1.83	186	foam	2.78	52.2	3.41
	4.648[a]	--	--		air[b]	3.49	0	--
13,120	4.597	6.01	2.85	335	ice	3.45	214	6.76
	4.597	5.97	2.85	334	foam	3.92	109	5.05
	4.661[a]	--	--	--	air[b]	6.36	0	--
13,136	4,597	6.73	3.24	428	ice	3.80	256	7.34
	4.618	6.88	3.22	434	foam	4.37	133	5.53
	4.623[a]	--	--	--	air[b]	7.60	0	--

a. Only free-surface velocity was measured on this sample.
b. Buffer was air, so particle velocity corresponds to free-surface velocity.

Table VI

RELEASE ADIABAT DATA FOR POLYCRYSTALLINE ICE

(Initial Density = 0.917 g/cm^3)

Shot No.	Sample Thickness (mm)	Hugoniot State			Release Adiabat States			
		Shock Velocity (mm/μsec)	Particle Velocity (mm/μsec)	Stress (kbar)	Buffer Material	Particle Velocity (mm/μsec)	Stress (kbar)	Shock Velocity in Buffer (mm/μsec)
13,119	4.623	4.98	2.22	101	foam	2.80	52.8	3.43
	4.496[a]	--	--	--	air[b]	3.70	0	--
13,097	4.610	6.69	3.35	206	foam	4.19	122	5.29
	4.623[a]	--	--	--	air[b]	6.04	0	--
13,140	4.577	7.48	3.88	266	foam	4.67	152	5.92
	4.590[a]	--	--	--	air[b]	7.10	0	--

a. Only free-surface velocity was measured on this sample.
b. Buffer was air, so particle velocity corresponds to free-surface velocity.

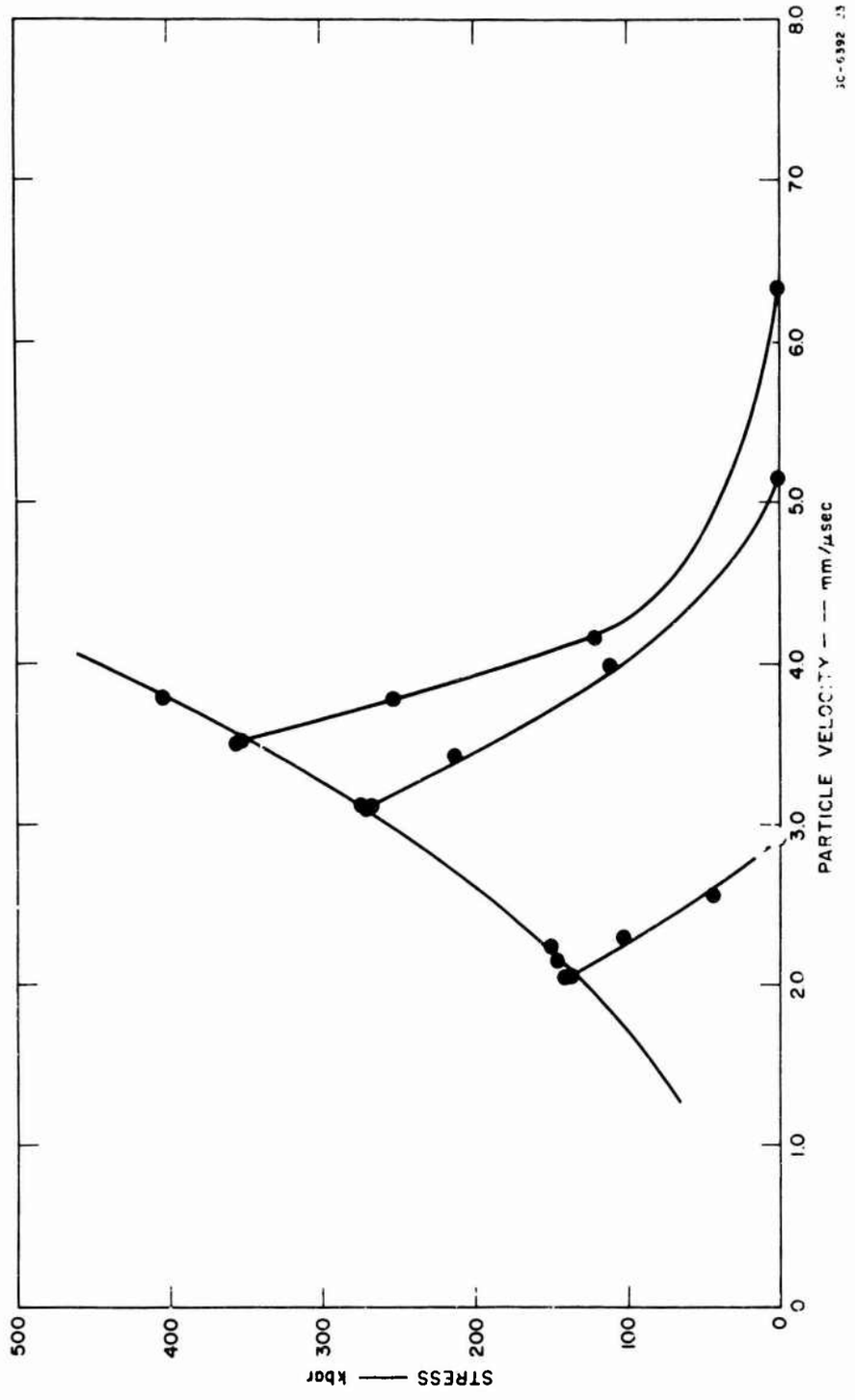

FIG. 21 HUGONIOT AND RELEASE CROSS CURVES FOR DRY OTTAWA BANDING SAND (σ -- u)

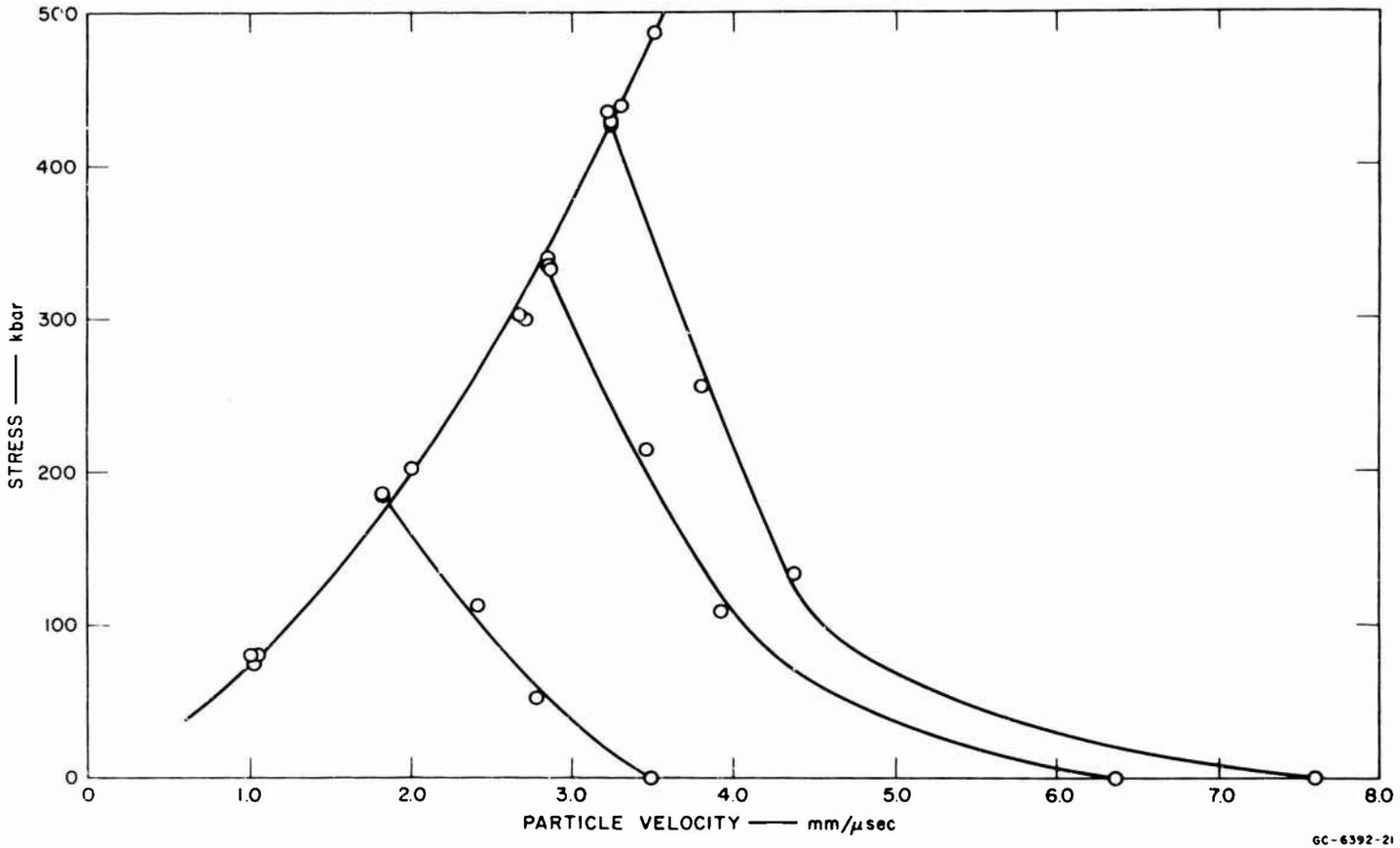

FIG. 22 HUGONIOT AND RELEASE CROSS CURVES FOR SATURATED OTTAWA BANDING SAND (σ – u)

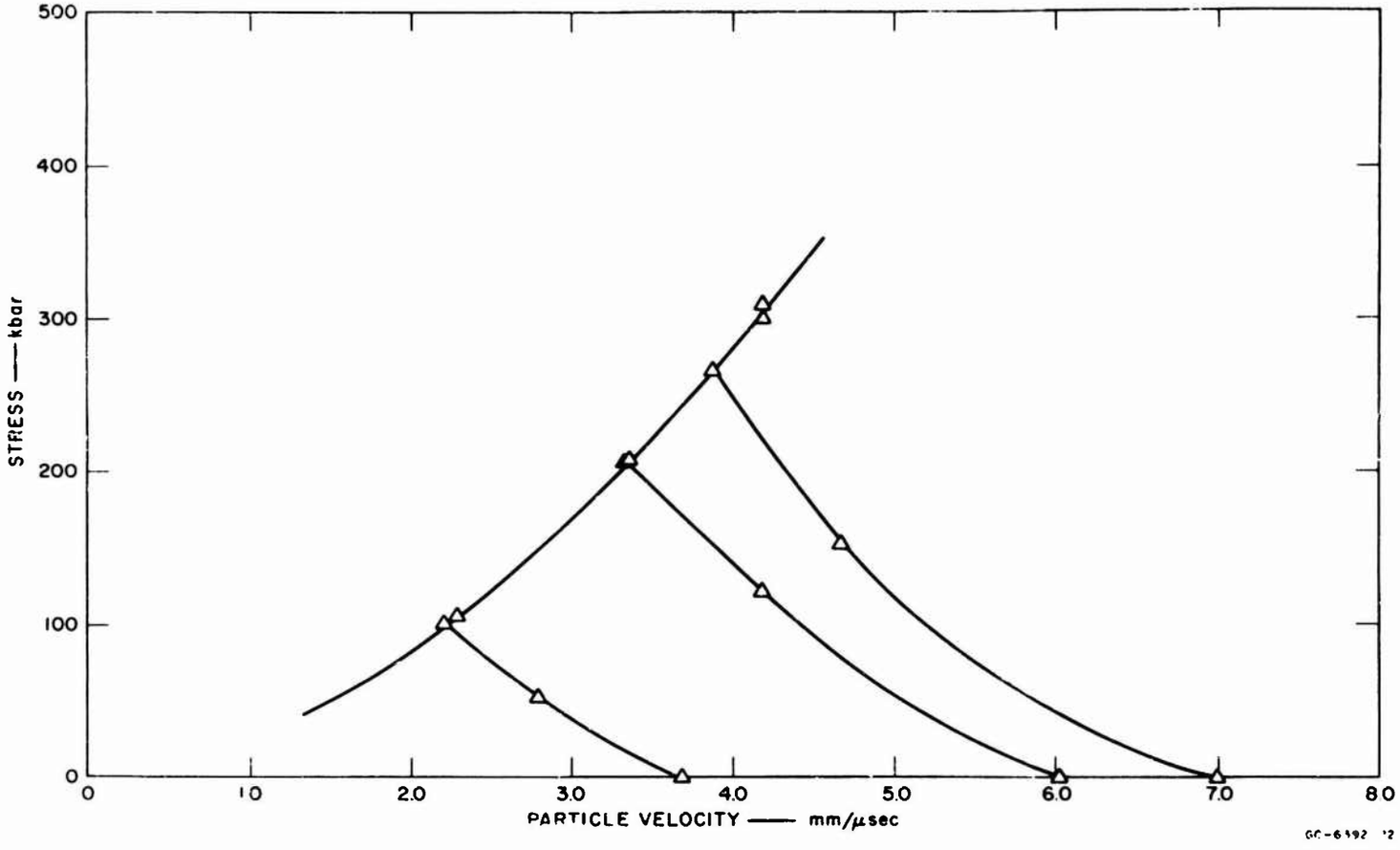

FIG. 23 HUGONIOT AND RELEASE CROSS CURVES FOR POLYCRYSTALLINE ICE (σ - u)

Dry Ottawa Sand. The cross curves for dry Ottawa sand (Fig. 21) are all steeper than the Hugoniot curve. This is to be expected, since the sand is initially porous and the shock process involves a great deal of irreversible crushing. The release cross curves for the dry sand are quite similar to those for polycrystalline quartz (Ahrens et al., 1966). The release curve from the high stress state is initially quite steep and then undergoes a rapid change in slope at some point below 100 kbar. Shock attenuation or a nonreversible phase change could produce this type of a cross curve. As discussed above, an effort was made to minimize shock attenuation, and although some attenuation may be present, it is not felt that this is the sole cause of the steep cross curve. Similar behavior is also observed in solid polycrystalline quartz shocked above 350 kbar (Ahrens et al., 1966). The high-density silica polymorph stishovite has been recovered from shock experiments on porous sandstone in which estimated stresses between 150 kbar and 300 kbar were achieved (DeCarli and Milton, 1965). This transformation is suggested as the possible cause for the steepness of the Hugoniots of the different sand samples above 300 kbar. If, upon release, the transformation of the high-density phase back into a low-density crystalline or glassy phase does not follow the decrease in stress and temperature due to the rarefaction, a steep release curve will result. It is suggested that this process was occurring and was responsible for the initial steepness of the high stress release cross curve of the dry sand.

Saturated Ottawa Sand. The cross curves for the saturated Ottawa sand (Fig. 22) show essentially the same characteristics as those of the dry sand. Because water was filling the pores, the shock impedance of the saturated sand was greater than that of the dry sand. The release cross curves are not as steep compared to the Hugoniot as they are in the case of dry sand. This is to be expected, since upon release the water expands the voids, whereas more permanent compaction takes place in dry sand. As in the case of dry sand, the release curve from the highest stress is initially quite steep. Another interesting feature of the release curves for saturated sand is the extremely high free-surface velocity associated with release from the intermediate and high stress states.

This high free-surface velocity implies a large final volume of the material upon release to zero stress. This behavior has been observed in other soils containing a large amount of water (Anderson et al., 1965). It appears that the shape of the upper portion of the two high stress release curves was influenced primarily by the silica, while the free-surface velocity was associated with the water. Assuming that the water and the silica sand were in stress equilibrium behind the shock, when the water was released to zero stress it would achieve a higher particle velocity, and this effect could produce the high free-surface velocity observed with the saturated sand.

Ice. The release cross curves for polycrystalline ice (Fig. 23) are less steep compared to the Hugoniot than those for the sand. This is to be expected since the ice underwent neither the irreversible compaction of the porous dry sand nor the polymorphic phase transition. However, the ice did undergo a 50% change in volume when shocked to the highest obtained stress, and quite possibly it vaporized (the energy increase was about 2100 cal/g). Therefore, the shock process was accompanied by a large increase in entropy and the cross curves would be expected to be quite different from mirror images of the Hugoniot. Notice in Fig. 23 that the free-surface velocity of the ice when shocked to 266 kbar was 7 mm/μsec. The saturated sand, when shocked to 466 kbar, had a free-surface velocity of 7.6 mm/μsec. On the basis of the present data, ice shocked to 466 kbar would be expected to exhibit a free-surface velocity much greater than 7.6 mm/μsec. Therefore, it appears that either the high free-surface velocity of the saturated sand was not due solely to the ice or that the ice and sand were not in stress equilibrium. In either case, the presence of water or ice in soil influences the release cross curve of the soil from high stresses in a manner so as to make the free-surface velocity greater than twice the particle velocity behind the initial shock.

SUMMARY AND RECOMMENDATIONS FOR FUTURE WORK

The Hugoniots of Ottawa sand and West Lebanon glacial till of various saturations have been quite well established over the stress range from about 60 to 500 kbar. The Hugoniots of single and polycrystalline ice have been established over the stress range from 35 to 300 kbar. No significant difference between the single and the polycrystalline ice was observed. Release cross curve data were also obtained for dry and saturated Ottawa sand and for polycrystalline ice. Both the Hugoniots and release cross curves for the soils became quite steep when the shock stress reached about 300 kbar. A plausible explanation for this behavior is that it is a manifestation of the quartz-stishovite phase transition. The release cross curves for ice were somewhat steeper than the Hugoniot, so that the free-surface velocity was less than twice the particle velocity.

For predicting wave propagation in the ground caused by an explosive source, knowledge of shock behavior in the low stress region is quite important. (By "low stress" is meant the stress region below, say, 30 kbar.) The ground near the source will be subjected to stresses of hundreds of kilobars, but as the pulse diverges the majority of the material affected will be subjected to much lower stresses. Of particular interest is the region in which the soil is only partially compacted. The phase changes in ice (ice I - ice II, ice I - ice III, etc.) may also affect the wave profile in the low stress region. There are considerable isothermal data for ice in this stress region. However, where phase changes occur, the shock behavior of a material may be quite different from the static behavior, due to the time scales associated with the shock process and the reaction kinetics. It is suggested, therefore, that further work to determine shock propagation and attenuation in frozen soils be directed at the low stress region.

REFERENCES

Ahrens, T. J., J. T. Rosenberg, and M. H. Ruderman (1966), Dynamic properties of rocks, Final Report SRI Project FGU-4816, Contract DA-49-146-X2-277, September 30, 1966.

Anderson, G. D., G. E. Duvall, J. O. Erkman, G. R. Fowles, and C. P. Peltzer, Investigation of the equation of state of porous earth media, AFWl-TR-65-146, Stanford Research Institute, July 1965.

Bethe, H. A. (1942), The theory of shock waves for an arbitrary equation of state, OSRD Report No. 545.

DeCarli, P. S., and D. J. Milton, Stishovite: synthesis by shock wave, Science 147, 144 (January 8, 1965).

Dorsey, E. N. (1940), Properties of ordinary water substance, Reinhold Publishing Corporation, New York.

Rice, M. H., R. G. McQueen, and J. M. Walsh (1958), Compression of solids by strong shock waves, Solid State Physics, Vol. 6, Academic Press, Inc., New York.

Unclassified

Security Classification

DOCUMENT CONTROL DATA - R & D

(Security classification of title, body of abstract and indexing annotation must be entered when the overall report is classified)

1. ORIGINATING ACTIVITY *(Corporate author)*
U.S. Army Cold Regions Research and Engineering Laboratory, Hanover, N. H.

2a. REPORT SECURITY CLASSIFICATION
Unclassified

2b. GROUP

3. REPORT TITLE
THE EQUATION OF STATE OF ICE AND COMPOSITE FROZEN SOIL MATERIAL

4. DESCRIPTIVE NOTES *(Type of report and inclusive dates)*
Research Report

5. AUTHOR(S) *(First name, middle initial, last name)*
Gordon D. Anderson

6. REPORT DATE	7a. TOTAL NO. OF PAGES	7b. NO. OF REFS
June 1968	57	6

8a. CONTRACT OR GRANT NO.	9a. ORIGINATOR'S REPORT NUMBER(S)
Contract DAAG 23-67-0011	Research Report 257
b. PROJECT NO.	
c. DA Task 1T025001A13001	9b. OTHER REPORT NO(S) *(Any other numbers that may be assigned this report)*
d.	

10. DISTRIBUTION STATEMENT
This document has been approved for public release and sale; its distribution is unlimited.

11. SUPPLEMENTARY NOTES	12. SPONSORING MILITARY ACTIVITY
Work performed by Stanford Research Institute, Menlo Park, California	Advanced Research Projects Agency

13. ABSTRACT

To compute shock wave propagation in frozen soil-water mixtures it is necessary to know a constitutive relation or an equation of state of the medium under consideration. Shock wave techniques provide a powerful tool for the investigation of equations of state at very high stress levels. The stress-volume behavior of frozen soil-water mixtures in the range from 60 to 500 kbar was investigated. Hugoniot data were obtained for Ottawa banding sand (pure quartz sand) and West Lebanon (New Hampshire) glacial till of varying degrees of saturation and for polycrystalline and monocrystalline ice (c-axis oriented in the direction of shock propagation). Release cross curve data were obtained for dry and saturated Ottawa banding sand and for polycrystalline ice. All materials were at an initial temperature of -10°C. In all experiments plane one-dimensional shock waves were used. The Hugoniots and release curves for the soil materials show evidence of a quartz-stishovite phase transition at about 300 kbar. The Hugoniots of single and polycrystalline ice do not differ significantly over the stress range studied – 30 kbar to 300 kbar.

DD FORM 1 NOV 68 1473 REPLACES DD FORM 1473, 1 JAN 64, WHICH IS OBSOLETE FOR ARMY USE.

Unclassified

Security Classification

14 KEY WORDS	LINK A		LINK B		LINK C	
	ROLE	WT	ROLE	WT	ROLE	WT
Shock waves Frozen soil Hugoniot						